4. Mechanics of Ocean Waves

James M. Kaihatu, Palaniswamy Ananthakrishnan

This chapter reviews mechanics of water waves and wave–body interactions pertaining to ocean and coastal engineering based on linear and weakly nonlinear wave theories. Numerical methods based on Green's theorem and mixed Eulerian–Lagrangian formulation for fully nonlinear wave and wave–body interaction problems are also discussed. The discussion also covers methods to determine the wave forces on fixed and floating structures, including the viscous drag force.

4.1 Ocean Surface Waves

The interface between the atmosphere and water, when disturbed, results in the generation of surface waves. In an open domain, the disturbance has to continue for the waves to persist as the propagating waves radiate energy. There is a limit to the energy contained by waves; once exceeded, wave breaking occurs, at which point energy is dissipated by turbulence during the breaking process. The limit depends on parameters such as wave height to wave length (or steepness) and wave height to water depth ratios. Wave instabilities or damping are also governed by air flow and separation, surface tension and surfactant effects, and instability of the free surface boundary layers. The physics of water waves is unique in many respects compared to other wave motions in fluids because of the dispersive nature of the water waves. Water wave problems are among the earliest topics attempted in applied mathematics, as illustrated, for example, by the classical Cauchy–Poisson problem on transient waves, tackled as early as in 1815 [4.1] and *Michell*'s theory of ship wave resistance developed in 1898 [4.2, 3]. A historical account of the development of classical water wave theory is given in [4.1]. Today, from an engineering viewpoint, understanding the properties of waves and wave–body

interactions is essential for efficient design and performance prediction of surface ships, offshore platforms, coastal structures, beach erosion mitigation measures, and beach fill configurations.

This chapter of the Handbook deals with the mechanics of surface waves, in particular:

1. Kinematic properties of surface waves
2. Weakly nonlinear deep water waves
3. Transformation of waves as they approach land from the deep ocean
4. Shallow water waves
5. Evolution of deep and shallow water waves
6. Breaking waves
7. Nearshore long wave generation, and
8. Wave forces on floating and fixed ocean structure.

Linear, weakly nonlinear, and fully nonlinear theories, and results on above topics are reviewed. The formulation of nonlinear wave theories in deep and shallow water are outlined, including the spectral evolution of these waves. Methods to solve wave–body interaction problems and to determine wave forces are discussed. The subject is presented in a manner so that it can serve as a reference for practicing engineers and researchers in ocean engineering. In each section of the chapter, an overview of the mathematical theory and formulations is given along with references for details.

4.2 Wave Theories

With exact equations governing water waves, wave transformations and wave–body interactions being nonlinear and involving arbitrary boundaries which make analysis difficult, numerous approximate theories have been developed over the years. These include linear Airy wave theory, Stokes weakly nonlinear theory, Boussinesq weakly nonlinear long wave theory and Korteweg–de Vries (KdV) theory for shallow water waves. Recent developments include computational methods to solve the fully nonlinear wave problem with the notable one by *Longuet-Higgins* and *Cokelet* based on mixed Eulerian–Lagrangian formulation [4.4].

Table 4.1 Key wave and flow variables

A	wave amplitude
C_g	wave group speed
C_p	wave phase speed
g	acceleration of gravity
h	water depth
H	wave height
k	wave number
L	wave length
p	pressure field
s	surface tension
t	time variable
T	wave period
$\boldsymbol{u}$	velocity field
(x, y, z)	Inertial earth-fixed coordinates against g with $z = 0$ on the calm surface
γ	specific weight of water
η	wave elevation
$\boldsymbol{\phi}$	velocity potential
ρ	water density
ω	wave radian frequency
$\boldsymbol{\Omega}$	vorticity

The above theories are based on the potential flow formulation, which assumes water to be inviscid and flow irrotational. The wave boundary conditions are, however, still nonlinear; they may be linearized for the case of small amplitude waves as in Airy's water wave theory. Despite the idealization and assumptions involved, linear theory captures many properties of wave phenomena and measures wave effects quite reasonably in most cases. Of course, for practical engineering applications, knowledge of large amplitude waves, including transformation over rapidly changing bathymetry, is essential; here linear theory has limited application and one has to consider weakly and fully nonlinear wave models. This chapter reviews these theories and the corresponding wave properties.

4.2.1 Potential Flow Formulation

We begin with a brief overview of the mathematical formulation of the water wave problem. The notations used in this chapter for key wave and flow variables are shown in Table 4.1. Additional notations used locally in the text are explained in the context.

A typical wave–body interaction and wave transformation problem encountered in ocean engineering and considered in this chapter is illustrated in Fig. 4.1. The body S_B may either be stationary or moving with velocity $\boldsymbol{U}$ (translation) and $\boldsymbol{\Omega}$ (rotational), resulting in a normal velocity $V_n = \boldsymbol{U} \cdot \hat{n} + \boldsymbol{\Omega} \cdot (\boldsymbol{r} \times \hat{n})$ with $\boldsymbol{r}$ denoting the position vector from the axis of rotation.

Neglecting effect of viscosity and consequently assuming the flow to be irrotational (i. e., $\boldsymbol{\omega} \equiv (\nabla \times \boldsymbol{u} = 0)$), one can define the flow in terms of velocity potential so that

$$\boldsymbol{u} = \nabla \boldsymbol{\phi} \, . \tag{4.1}$$

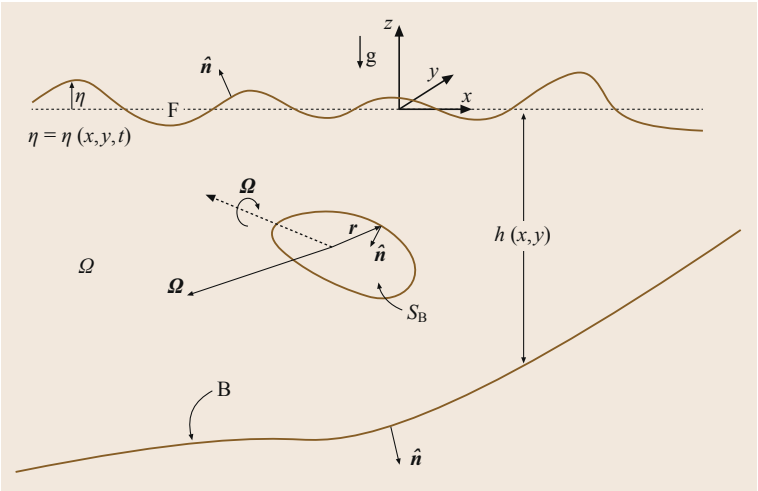

Fig. 4.1 Illustration of wave–body interaction and wave transformation over changing bathymetry

For incompressible fluid, per equation of continuity,

$$\nabla \cdot \boldsymbol{u} = 0\,, \tag{4.2}$$

which in terms of $\boldsymbol{\phi}$ is the Laplace equation

$$\nabla^2 \boldsymbol{\phi} = 0\,. \tag{4.3}$$

With $\boldsymbol{u} = \nabla\boldsymbol{\phi}$ in the Euler equation motion and through spatial integration one obtains the following Euler's integral for the pressure

$$p = -\rho g z - \rho \frac{\partial \boldsymbol{\phi}}{\partial t} - \frac{\rho}{2}|\nabla \boldsymbol{\phi}|^2, \tag{4.4}$$

with the first term on the right-hand side representing the static pressure and the last two terms denoting the dynamic pressure.

The bottom and body boundary conditions are the no-flux conditions given by

$$\frac{\partial \boldsymbol{\phi}}{\partial n} = 0, \quad \text{on the bottom B}\,, \tag{4.5}$$

and

$$\frac{\partial \boldsymbol{\phi}}{\partial n} = V_n, \quad \text{on the body surface } S_B\,. \tag{4.6}$$

On the free surface, we have the following two conditions, one based on the kinematics of free surface motion and the other on the continuity of pressure across the free surface

$$\frac{\partial \eta}{\partial t} + \frac{\partial \eta}{\partial x}\frac{\partial \boldsymbol{\phi}}{\partial x} + \frac{\partial \eta}{\partial y}\frac{\partial \boldsymbol{\phi}}{\partial y} = \frac{\partial \boldsymbol{\phi}}{\partial z} \quad \text{on } z = \eta\,, \tag{4.7}$$

$$\frac{\partial \boldsymbol{\phi}}{\partial t} + \frac{1}{2}|\nabla \boldsymbol{\phi}|^2 + g\eta = 0, \quad \text{on } z = \eta\,. \tag{4.8}$$

The former is called the free surface kinematic condition and the latter the free surface dynamic condition. Both are specified on $z = \eta$, which in itself is also an unknown and to be solved as a part of the problem. These conditions make the problem nonlinear and, therefore, difficult to solve.

For small amplitude waves (i. e., one in which the wave amplitude is much smaller than the wave length), the free surface boundary conditions can be linearized as

$$\frac{\partial \eta}{\partial t} + \frac{\partial \boldsymbol{\phi}}{\partial z} \quad \text{on } z = 0\,, \tag{4.9}$$

$$\frac{\partial \boldsymbol{\phi}}{\partial t} + g\eta = 0 \quad \text{on } z = 0\,. \tag{4.10}$$

Eliminating η from the above two conditions, one obtains the following linearized combined free surface condition

$$\frac{\partial^2 \boldsymbol{\phi}}{\partial t^2} + g\frac{\partial \boldsymbol{\phi}}{\partial z} = 0 \quad \text{on } z = 0\,. \tag{4.11}$$

In the case of spatially periodic waves with wave length L in, say, x direction, $\boldsymbol{\phi}(x,y,z,t) = \boldsymbol{\phi}(x \pm nL, y, z, t)$ and $\eta(x,y,t) = \eta(x \pm nL, y, t)$ and for time harmonic case with period T, $\boldsymbol{\phi}(x,y,z,t) = \boldsymbol{\phi}(x,y,z,t \pm nT)$ and $\eta(x,y,t) = \eta(x,y,t \pm nT)$ where n denotes positive integer. The wave length L and wave period T are related by the dispersion relation as discussed later in the chapter.

4.3 Properties of Small Amplitude Gravity Waves

In the absence of a body in the fluid, a periodic two-dimensional (long crested) progressive small amplitude (linear) wave solution to the linearized problem (as formulated above) can be written as

$$\phi = \frac{H}{2}\frac{\mathrm{g}}{\omega}\frac{\cosh k(z+h)}{\cosh kh}\sin(kx-\omega t)\,,$$
$$\eta = \frac{H}{2}\cos(kx-\omega t)\,, \tag{4.12}$$

where $k \equiv 2\pi/L$ denotes the wave number, H the wave height (which the vertical distance between the crest and trough), and h the mean water depth (taken here to be constant). In the case of a deep water wave, i. e., in the limit $kh \to \infty$ with $z \in [0, -h]$ the above solution becomes

$$\phi = \frac{H}{2}\frac{\mathrm{g}}{\omega}\mathrm{e}^{kz}\sin(kx-\omega t)\,,$$
$$\eta = \frac{H}{2}\cos(kx-\omega t)\,. \tag{4.13}$$

For the above velocity potential, the velocity field ($\boldsymbol{u} = \nabla\phi$) is given by

$$u = \frac{H}{2}\mathrm{g}k\omega\frac{\cosh k(z+h)}{\cosh kh}\cos(kx-\omega t)\,,$$
$$v = 0\,,$$
$$w = \frac{H}{2}\mathrm{g}k\omega\frac{\sinh k(z+h)}{\cosh kh}\sin(kx-\omega t)\,.$$

From above expressions one finds that the horizontal velocity field is in phase with the wave elevation. Its slip on the bottom is to be interpreted as the velocity at the outer edge of a bottom boundary layer. Using the Euler integral one can obtain the following expression for the pressure

$$p = -\rho\mathrm{g}z + \rho\mathrm{g}\frac{H}{2}\frac{\cosh k(z+h)}{\cosh kh}\cos(kx-\omega t)$$
$$= -\rho\mathrm{g}z + \rho\mathrm{g}\eta\frac{\cosh k(z+h)}{\cosh kh}\,.$$

In the case of shallow water waves – i. e., for $kh \to 0$ with $z \in [0, -h]$ (or approximately, $kh \le \pi/10$) –, the expression for pressure reduces to

$$p = -\rho\mathrm{g}(z-\eta).$$

The above expression looks very similar to the familiar hydrostatic pressure equation for homogeneous water. The static pressure corresponds to the depth measured from the calm surface while total pressure to the depth measured from the actual free surface with the difference contributes to the dynamic pressure.

4.3.1 Linear Dispersion Relation

As per the linear solution obtained above, the wave number $k \equiv 2\pi/L$ and wave frequency $\omega \equiv 2\pi/T$ are related by the dispersion relation

$$\omega^2 = \mathrm{g}k\,\tanh kh\,, \tag{4.14}$$

which approximates to

$$\omega^2 = \mathrm{g}k,\ \text{for}\ kh \ge \pi\,, \tag{4.15}$$

and to

$$\omega^2 = \mathrm{g}k^2h,\ \text{for}\ kh \le \pi/10\,. \tag{4.16}$$

The dispersion relation thus provides a basis for defining deep water, shallow water, and intermediate waves. Waves satisfying $kh \ge \pi$, which is the same as $h \ge L/2$, are referred to as deep water (or short) waves; that satisfying $kh \le \pi/10$, which is same as $L \ge 20h$, are referred to as shallow water (or long) waves and that in between (i. e., $\pi/10 < kh < \pi$) as the intermediate waves.

4.3.2 Phase Speed

The phase speed (also known as the wave speed or wave celerity) for linear waves becomes

$$C_\mathrm{p} \equiv \frac{L}{T} = \frac{\omega}{k} = \sqrt{\frac{\mathrm{g}}{k}\tanh kh}\,, \tag{4.17}$$

which reduces to

$$C_\mathrm{p} = \sqrt{\frac{\mathrm{g}}{k}\tanh kh}, \text{for}\ \pi/10 < kh < \pi$$
(intermediate waves)
$$= \sqrt{\frac{\mathrm{g}}{k}}, \text{for}\ kh \ge \pi$$
(deep water or short waves)
$$= \sqrt{\mathrm{g}h}, \text{for}\ kh \le \pi/10$$
(shallow water or long waves)\,. \tag{4.18}

As can be observed in the above expressions, longer deep water waves travel faster. In the case of shallow water waves the wave speed depends only on the local depth; the phase speed decreases with decreasing depth.

4.3.3 Group Speed

Often it is the group speed that govern many important wave properties, including the speed of energy propa-

gation, among others. The group speed is defined as

$$C_g \equiv \frac{d\omega}{dk}\,, \tag{4.19}$$

which in view of the dispersion relation for linear gravity waves become

$$\begin{aligned} C_g &= \frac{\omega}{2k}\left(1+\frac{2kh}{\sinh 2kh}\right), \text{ for } \pi/10 < kh < \pi \\ &= \frac{\omega}{2k} = \frac{C_p}{2} = \frac{1}{2}\sqrt{\frac{g}{k}}, \text{ for } kh \geq \pi \\ &\quad \text{(deep water waves)} \\ &= \frac{\omega}{k} = C_p = \sqrt{gh}, \text{ for } kh \leq \pi/10 \\ &\quad \text{(shallow water waves)}\,. \end{aligned} \tag{4.20}$$

So, for linear gravity waves, except in the limit of shallow water (long) waves, the group speed is different from the phase speed, and this fact has a bearing on some unique properties of shallow water waves to be discussed in later sections.

4.3.4 Amplitude Modulation of Water Waves

A wave consisting of two periodic progressive waves of equal amplitude and nearly equal wave number, and because of the continuous dispersion relation nearly equal frequency, will undergo an amplitude modulation with the modulation itself propagating as a wave but at the group speed rather than the phase speed. In other words,

$$\begin{aligned} \eta &= \eta_1 + \eta_2 \\ &= \frac{H}{2}\cos(k_1 x - \omega_1 t) + \frac{H}{2}\cos(k_2 x - \omega_2 t)\,, \\ &\quad \text{where } k_1 = k + \frac{\delta k}{2},\ k_2 = k - \frac{\delta k}{2}, \\ &= H\ \cos(\delta k\, x - \delta\omega\, t)\ \cos(kx - \omega t), \\ &\quad \omega_1 = \omega + \frac{\delta\omega}{2},\ \omega_2 = \omega - \frac{\delta\omega}{2}, \\ &= A\ \cos(kx - \omega t), \\ &\quad \text{where the amplitude } A \equiv H\ \cos(\delta k\, x - \delta\omega\, t)\,. \end{aligned} \tag{4.21}$$

The amplitude envelope propagates at speed $\delta\omega/\delta k$ and in the limit of $\delta\omega, \delta k \to 0$, at the group speed C_g! To an observer moving in the direction of wave propagation, the amplitude will appear stationary (constant); however, the observer will not be in phase with the wave, unless if it is a shallow water wave in which case $C_g = C_p$. Thus we observe that in the case of amplitude-modulated waves, the wave amplitude is conserved at the group speed.

4.3.5 Average Wave Energy Density

Through straightforward integration and averaging over a wave period, it can be shown that the average wave potential energy in a water column of unit cross area is given by

$$\overline{PE} = \frac{1}{16}\rho g H^2\,.$$

The word *density* in the present context corresponds to the unit area of the cross-section of the water column. Similarly, using the expressions for velocity and the definition of kinetic energy one can show that the average wave kinetic energy density is given by

$$\overline{KE} = \frac{1}{16}\rho g H^2\,,$$

and, therefore, the average wave mechanical energy density

$$\bar{E} \equiv \overline{PE} + \overline{KE} = \frac{1}{8}\rho g H^2\,.$$

To particularly note in the above expression is the fact that the wave energy is proportional to the square of the wave height.

4.3.6 Propagation of Wave Energy

Using the work-energy theorem, it can be shown that the average amount of energy propagating across a surface of unit crest length is given by

$$\bar{\mathcal{F}} = \bar{E} C_g\,,$$

meaning that the wave energy propagates at the group speed! For example, in the case of a wave front advancing in deep water the waves will appear to disappear at the wave front because $C_p = 2C_g$; in other words, propagation of energy cannot keep up with phase to sustain the wave. The above expression is quite useful to estimate the power required to generate waves and the wave resistance of vehicles moving over a free surface and wave energy conversion. In the case of confluence or divergence of waves, as due to bottom bathymetry or power take off, one has to multiply the above expression by the respective crest widths. The reader may refer to the topic of the *antenna effect* in the chapter on wave energy conversion of this Handbook for more on this aspect.

4.3.7 Water Particle Trajectory

For a propagating wave with velocity known (from above) one can determine the trajectory of water particles through time integration. For small amplitude waves, the trajectory is elliptical and closed

$$\frac{(X-X_o)^2}{A^2}+\frac{(Z-Z_o)^2}{B^2}=1\,,$$

where (X_o, Z_o) denote the coordinates of the center of the ellipse, A the major semi-axis

$$A\equiv\frac{H}{2}\frac{gk}{\omega^2}\frac{\cosh k(Z_o+h)}{\cosh kh}\,,$$

and B the minor semi-axis

$$B\equiv\frac{H}{2}\frac{gk}{\omega^2}\frac{\sinh k(Z_o+h)}{\cosh kh}\,.$$

As to be expected, near the bottom the particle will oscillate back and forth parallel to the bottom. In the case of deep water waves ($kh\to\infty$, or for practical calculations $kh\geq\pi$), above expressions for semi-axes reduce to

$$A=B=\frac{H}{2}\frac{gk}{\omega^2}e^{kZ_o}=\frac{H}{2}e^{kZ_o}\,.$$

In other words, the trajectory is a circle for small amplitude deep water waves. As the particle paths are closed, the average mass transport is zero. However, in the case of finite amplitude waves, this is not the case. In the case of finite amplitude waves, the trajectory is not quite closed, meaning that a particle will not return to the original position after one wave period but to a point slightly ahead of the original point. This is referred to as the Stokes drift. More on finite amplitude wave properties are given in later sections of this chapter.

4.3.8 Spatio-Temporal Evolution of Waves

Consider the generation of waves by (for example) a mudslide into water or by a seismic activity and the resulting waves propagating over water of varying depth. Here both wave numbers and frequency will vary with space and time. Let the direction of the wave propagation be along the x direction. Here the wave number and frequency may vary both in x and in time. In other words, the phase function will be

$$\Theta=(k(x,t)x-\omega(x,t)t)\,.$$

With the so-called slowly varying wave assumption, the wave number and wave frequency can be written as

$$k\approx\frac{\partial\Theta}{\partial x};\ \omega\approx-\frac{\partial\Theta}{\partial t}\,.$$

Cross-differentiating the above expressions we obtain

$$\frac{\partial k}{\partial t}+\frac{\partial\omega}{\partial x}=\frac{\partial^2\Theta}{\partial x\partial t}-\frac{\partial^2\Theta}{\partial t\partial x}=0\,. \tag{4.22}$$

In the special case of the steady-state limit, i. e., $k=k(x)$ and $\omega=\omega(x)$, from above we find ω to be constant. Thus, in the case of steady-state evolution of waves, the wave number (hence wave length) may change spatially in x, but the frequency will be the same everywhere.

The above equation for k and ω can be re-written as

$$\frac{\partial k}{\partial t}+C_g\frac{\partial k}{\partial x}=0,\ \text{where } C_g=\text{Group Speed}=\frac{d\omega}{dk}\,. \tag{4.23}$$

The above equation is called the wave number conservation equation; its solution implies that k will appear constant to an observer moving at the group speed. One could draw several other important conclusions using this equation. For example, assume waves are propagating in deep water (i. e., so that $kh\geq\pi$). At a fixed field point away from the wave source, as per the wave number conservation equation, the wave frequency and wave number will increase with respect to time, meaning that as time progresses shorter and shorter waves will reach the field point. To deduce this fact from the wave number conservation equation, consider the time that will be taken by a wave of wave number k generated at the source to reach the field point

$$t=\frac{d}{C_g}\ \to\ C_g=\frac{d}{t}\,,$$

where d denotes the distance between the source and the field point. Since $C_g=0.5\,g/\omega$ for deep water gravity waves, the above becomes

$$\frac{1}{2}\frac{g}{\omega}=\frac{d}{t}\to\omega=\frac{1}{2}\frac{gt}{d}\,.$$

In other words, the frequency of waves reaching the field point increases as the time increases. With $\omega^2=gk$ for deep water waves, the above equation can be written as

$$k=\frac{1}{4}\frac{gt^2}{d^2}\,,$$

meaning that the number of waves reaching the field point will also increase with time.

4.3.9 Shoaling and Refraction of Waves

One can generalize the derivations and findings of the previous section to allowing the waves to propagate along any arbitrary direction. In the case of slowly varying, small amplitude steady-state waves approaching an ideal coast (straight and long shore line with all bottom bathymetry contours parallel to the shore line) the direction of wave propagation is governed by Snell's law

$$\frac{\sin\theta}{C_\mathrm{p}} = \text{constant}\,, \tag{4.24}$$

where θ denotes the local angle of wave incidence measured from the shore normal, with $\theta = 0$ corresponding to crests parallel to the shore and $\theta = 90°$ to crests normal to the shore. The change of direction of wave propagation is called wave refraction. As one may recall from classical physics, the path of waves as predicted by the above Snell's law corresponds to the shortest time of travel between two points in a variable velocity field. If the velocity is constant, then θ will also be constant, meaning that the path of wave propagation will be a straight line.

As the waves approach the shore with depth $h \to 0$, $C_\mathrm{p} \to \sqrt{gh} \to 0$, then θ should also $\to 0$ for the ratio $\frac{\sin\theta}{C_\mathrm{p}}$ to remain constant; in other words, the wave rays will be normal to the shoreline irrespective of the angle of incidence of the wave while offshore.

Note that in the case of slowly varying steady-state waves, the wave frequency will remain constant and the wave number evolve satisfying the dispersion relation

$$gk\tanh kh = \text{constant}\,.$$

Assuming no wave breaking (which would enhance dissipation through turbulence) and with conservation of mechanical energy, one can show that in the case of a slowly varying, steady-state, nonbreaking wave approaching an ideal shore, the wave height will vary, satisfying

$$H\sqrt{\cos\theta}\,\sqrt{C_\mathrm{g}} = \text{constant} \;\to\; H = \frac{\text{constant}}{\sqrt{C_\mathrm{g}\,\cos\theta}}\,. \tag{4.25}$$

4.3.10 Closing Remarks to the Section

The linear (Airy) wave theory enables us to understand the basic and unique properties of surface waves. There are several books that deal with the linear theory of water waves, which the reader may refer to for details. These include [4.5–9]. The linear potential flow theory will hold good only for small amplitude waves. For finite and large amplitude waves, one has to use weakly and fully nonlinear wave theories, as reviewed in the following sections.

4.4 Weakly Nonlinear Deep Water Wave Theories

While linear theory has proved to be quite useful, it is often insufficient to investigate many of the details of wave propagation. Bulk properties of waves (some measure of wave height) are generally well predicted by linear theory in many instances. However, the small amplitude assumption inherent in linear wave theory is often invalidated (when waves approach their breaking condition), so nonlinear wave theory becomes essential.

The nonlinearity in water wave theory arises from the treatment of the surface boundary conditions. The kinematic and dynamic free surface boundary conditions are both nonlinear (they involve the products of the dependent variables $\boldsymbol{\phi}$ and η) and apply at a surface whose position is unknown a priori, as mentioned above. To move beyond simple linearization of the free surface condition (which involves neglecting the nonlinear terms and applying the boundary conditions on the surface $z = 0$), successive approximations to the nonlinear boundary conditions are required. This requires the establishment of physical scales, which become the basis of these approximations.

We first discuss deep water nonlinear wave theory, or Stokes wave theory (Stokes [4.10]). In deep water, the relative depth kh (where k is the wave number and h the water depth) is large. This can be used to adjust the velocity potential toward its deep water asymptote

$$\boldsymbol{\phi} = \frac{H}{2}\frac{\mathrm{g}}{\omega}\frac{\cosh k(z+h)}{\cosh kh}\sin(kx-\omega t) \approx \frac{\mathrm{g}H}{2\omega}\times O(1)\,, \tag{4.26}$$

which reflects the observation that the hyperbolic cosine term approaches 1 as kh becomes large. The particle velocities u and w similarly become

$$u = \frac{\partial\boldsymbol{\phi}}{\partial x} = \frac{\mathrm{g}kH}{2\omega}\frac{\cosh k(z+h)}{\cosh kh}\cos(kx-\omega t) \approx \frac{\mathrm{g}ka}{\omega}\times O(1) = \frac{\mathrm{g}\epsilon}{\omega}\times O(1)\,, \tag{4.27}$$

$$w = \frac{\partial \phi}{\partial z} = \frac{gkH}{2\omega}\frac{\sinh k(z+h)}{\cosh kh}\sin(kx-\omega t) \approx \frac{gka}{\omega}\times O(1) = \frac{g\epsilon}{\omega}\times O(1)\,, \tag{4.28}$$

where $\epsilon = ka$ and where the amplitude $a = H/2$. It is evident that both u and w are of the same scale of variation, and as such there is no separation between the horizontal and vertical length scales. This allows both the horizontal and vertical scales to be the same. The time variable is scaled using the deep water approximation to the linear dispersion relation. These scales are then applied to the water wave boundary value problem. While the governing equation and bottom boundary conditions remain unchanged, the free surface boundary conditions are transformed to reflect this new scaling. The dynamic free surface boundary condition is now

$$g\eta + \frac{\partial \phi}{\partial t} + \frac{\epsilon}{2}\left[\left(\frac{\partial \phi}{\partial x}\right)^2 + \left(\frac{\partial \phi}{\partial z}\right)^2\right] = 0 \quad \text{on } z = \epsilon\eta\,, \tag{4.29}$$

and the kinematic free surface boundary condition is

$$\frac{\partial \eta}{\partial t} - \frac{\partial \phi}{\partial z} + \epsilon\frac{\partial \eta}{\partial x}\frac{\partial \phi}{\partial x} = 0 \quad \text{on } z = \epsilon\eta\,, \tag{4.30}$$

(It is noted that these boundary conditions are expressed in dimensional form, with the small parameter ϵ modifying the free surface elevation variable η). We further use Taylor series expansion about $z = 0$, which generates additional powers of ϵ. The dynamic free surface boundary condition would then become

$$g\eta + \frac{\partial \phi}{\partial t} + \frac{\epsilon}{2}\left[\left(\frac{\partial \phi}{\partial x}\right)^2 + \left(\frac{\partial \phi}{\partial z}\right)^2\right] + \epsilon\eta\frac{\partial}{\partial z}\left\{g\eta + \frac{\partial \phi}{\partial t} + \frac{\epsilon}{2}\left[\left(\frac{\partial \phi}{\partial x}\right)^2 + \left(\frac{\partial \phi}{\partial z}\right)^2\right]\right\} + \ldots \text{ on } z = 0\,, \tag{4.31}$$

and the kinematic free surface boundary condition

$$\frac{\partial \eta}{\partial t} - \frac{\partial \phi}{\partial z} + \epsilon\frac{\partial \phi}{\partial x}\frac{\partial \eta}{\partial x} + \epsilon\eta\frac{\partial}{\partial z}\left(\frac{\partial \eta}{\partial t} - \frac{\partial \phi}{\partial z} + \epsilon\frac{\partial \phi}{\partial x}\frac{\partial \eta}{\partial x}\right) + \ldots \text{ on } z = 0\,. \tag{4.32}$$

Finally the dependent variables ϕ and η are expanded in a power series in terms of the parameter ϵ

$$\phi = \sum_{n=1}^{\infty}\epsilon^{n-1}\phi_n = \phi_1 + \epsilon\phi_2 + \ldots\,, \tag{4.33}$$

$$\eta = \sum_{n=1}^{\infty}\epsilon^{n-1}\eta_n = \eta_1 + \epsilon\eta_2 + \ldots\,, \tag{4.34}$$

and substituted into the boundary value problem. The problem can then be separated into orders and solved sequentially. The order of the theory is denoted by the parameter ϵ; second-order Stokes theory retains terms up to $O(\epsilon)$, third-order Stokes theory up to $O(\epsilon^2)$, etc. The solutions at each higher order are dependent on lower-order solutions.

4.4.1 Properties of Weakly Nonlinear Deep Water Waves

The solution for ϕ at second order in ϵ can be found to be

$$\phi = Kx + \frac{gH}{2\omega}\frac{\cosh k(h+z)}{\cosh kh}\sin(kx-\omega t) + \frac{3\omega H^2}{32\sinh^4 kh}\cosh 2k(h+z)\sin 2(kx-\omega t)\,, \tag{4.35}$$

where $Kx = U$ is a mean current that accounts for any nonperiodic components of the solution (this is quantified below), and

$$\eta = \frac{H}{2}\cos(kx-\omega t) + \frac{kH^2\cosh kh(2\cosh^2 kh+1)}{16\sinh^3 kh}\cos 2(kx-\omega t) - \frac{kH^2}{8\sinh 2kh}\,. \tag{4.36}$$

It can be seen that the free surface elevation is comprised of a fundamental (or first harmonic) oscillating at a frequency ω, a second harmonic component oscillating at a frequency 2ω, and a mean set down. The two oscillating components are in phase at the crests and 180° out of phase at the troughs; this has the effect of sharpening the crests and flattening the troughs of the combined Stokes wave. The mean set down arises due to the choice of the Bernoulli constant to equal zero, and in this instance is relevant to the case of waves propagating up a slope in an otherwise infinite ocean.

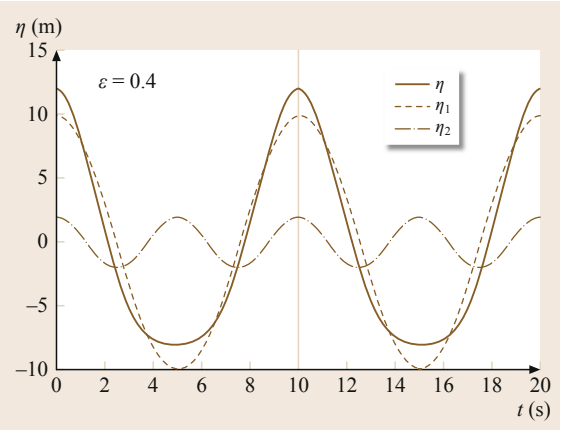

Fig. 4.2 Free surface of a second-order Stokes wave with $T = 10\ s$, along with the two component waves

However, for situations in which the motion is restricted to a finite domain (e.g., standing waves in a basin) the mean sea surface is necessarily zero, which would lead to a nonzero Bernoulli constant. Figure 4.2 shows the individual components and the total free surface profile for a second-order Stokes wave.

The particle velocities under a second-order Stokes wave can be derived from the velocity potential

$$u = \frac{\partial \phi}{\partial x} = K + \frac{gHk}{2\omega}\frac{\cosh k(h+z)}{\cosh kh}\cos(kx-\omega t) + \frac{3\omega H^2 k}{16\sinh^4 kh}\cosh 2k(h+z)\cos 2(kx-\omega t)\ , \tag{4.37}$$

$$w = \frac{\partial \phi}{\partial z} = \frac{gHk}{2\omega}\frac{\sinh k(h+z)}{\sinh kh}\sin(kx-\omega t) + \frac{3\omega H^2 k}{16\sinh^4 kh}\sinh 2k(h+z)\sin 2(kx-\omega t)\ . \tag{4.38}$$

The dispersion relation remains that of linear theory; the effects of nonlinearity on the wavelength appear at third order. Integrating the horizontal velocity u over depth and averaging over a wave period will allow an evaluation of the net mass flux (or Stokes drift). The value of the constant K is dictated by whether zero mass flux is indicative of the scenario at hand. For a large domain, the constant $K = 0$ and the mass flux is the value of the Stokes drift, while in confined situations the mass flux is necessarily zero and the mass flux would be carried by K. This also has implications for the definition of the phase speed C:

- The phase speed C can be defined as the speed of the wave relative to a stationary water column. In this case, $K = 0$, there is no net motion below the trough, and the phase speed

$$C = \sqrt{\frac{g}{k}\tanh kh}\ .$$

  The Stokes drift defines the net mass flux in the direction of wave propagation.
- The phase speed C can alternatively be defined as the speed of the wave relative to a stationary observer seeing waves with no mass flux. The phase speed would then be reduced by an amount proportional to the Stokes drift.

The pressure in the water column can be derived from the Bernoulli equation, and is

$$p = -\rho g z + \frac{\rho g H}{2}\frac{\cosh k(h+z)}{\cosh kh}\cos(kx-\omega t) - \frac{\rho g k H^2}{16\sinh kh\cosh kh}\cosh 2k(h+z) + \left[\frac{3\rho g k H^2}{16\cosh kh\sinh^3 kh}\cosh 2k(h+z) - \frac{\rho g h H^2}{16\sinh kh\cosh kh}\right]\cos 2(kx-\omega t)\ . \tag{4.39}$$

It is evident that the pressure contains a term that does not oscillate and another that is constant with depth. Evaluation of the pressure at the bottom ($z = -h$) reveals a term that reduces the static pressure due to the mean set down.

The basis of Stokes wave theory is that each harmonic of the fundamental frequency represents an additional order in the theory, and as such each harmonic amplitude becomes correspondingly smaller. It is difficult to establish a shallow water limit on the validity of Stokes theory based on the mathematical development, though a limit can be established on physical grounds. For example, one criterion could be that the second-order amplitude remain sufficiently small so that a bump does not appear in the trough of the wave; this implies that

$$kh > \sqrt{\frac{3a}{h}}\ , \tag{4.40}$$

for a bump to not appear in the trough.

4.4.2 Evolution of Weakly Nonlinear Deep Water Waves

Weakly nonlinear, deep water waves do not generally travel as permanent form waves, but evolve as a result of interactions with other waves of different frequencies and directions. These interactions can consist of

so-called *bound* waves (forced waves that do not satisfy the linear dispersion relation and, thus, can grow only a limited amount) and *resonant* waves (forced waves that do satisfy the linear dispersion relation and are thus able to grow without bound as the forcing is secular).

The expansion of the surface boundary conditions in powers of ϵ leads to products of unknowns that increase as the order of the expansion increases. Thus, given

$$\eta \approx e^{i\psi}, e^{-i\psi} , \tag{4.41}$$

(where $\psi = \mathbf{k}\cdot\mathbf{x} - \omega t$), higher-order terms lead to

$$\eta^2 \approx e^{2i\psi}, 1, e^{-2i\psi} , \tag{4.42}$$

$$\eta^3 \approx e^{3i\psi}, e^{i\psi}, e^{-i\psi}, e^{-3i\psi} , \tag{4.43}$$

and so on, until the desired truncation. Terms that result from this operation will remain bound to the primary harmonic and not experience unbounded growth. However, the η^2 will also generate terms proportional to $e^{i\psi}$ and $e^{-i\psi}$, and η^3 will generate terms proportional to $e^{2i\psi}$, 1, and $e^{-2i\psi}$, or (in both cases) terms proportional to the next lower-order solution. Solution of the resulting boundary value problem will generate terms that will grow linearly in either space or time without bounds (secular behavior). To ameliorate this, the method of multiple scales is often used to treat these problems. The application of this method allows the potentially secular behavior to be split into motions with different degrees of variation. In many cases, the fast degree of variation is associated with the waveform itself (the periodic motion) and the slow degree of variation with another property of the wave (for example, the amplitude of the wave form), which can then be linked to variations in some external field (e.g., the bathymetry).

The formalism in the previous section is most relevant to the case where a single wave component gives rise to harmonics, all of which can evolve during propagation to comprise a changing wave form. A coordinate system moving with the group velocity of the wave is defined; the resulting coordinates are defined as τ (time coordinate defining the slow temporal variation) and ξ (space coordinate defining the slow spatial variation). Carrying this analysis to third order will lead to the cubic nonlinear Schrödinger equations [4.11]

$$-i\frac{\partial A}{\partial \tau} - \frac{1}{2}\frac{\partial^2 \omega}{\partial k^2}\frac{\partial^2 A}{\partial \xi^2} + \beta|A|^2 A + \gamma A = 0 , \tag{4.44}$$

where

$$\beta = \frac{\omega k^2}{2} D + \frac{g^2 k^2}{2\omega(C_g^2 - gh)}\left(1 + \frac{kC_g}{2\omega\cosh^2 kh}\right)^2 , \tag{4.45}$$

and

$$\gamma = kS(\tau)\left(1 + \frac{kC_g}{2\omega\cosh^2 kh}\right) , \tag{4.46}$$

where $S(\tau)$ is an integration constant, and

$$D = \frac{\cosh 4kh + 8 - 2\tanh^2 kh}{8\sinh^4 kh} . \tag{4.47}$$

However, in most cases in the ocean, a description of wave propagation via the harmonics of a single wave is inapplicable, and we must turn toward a description comprised of a summation of waves of different frequencies and directions with random phases

$$\boldsymbol{\phi} = \sum_{n=1}^{\infty} -\frac{i}{2} B_n \frac{\cosh k_n(h+z)}{\cosh k_n h} e^{i(\mathbf{k_n}\cdot\mathbf{x} - \omega_n t + \epsilon_n)} + c.c. , \tag{4.48}$$

where B_n is the (complex) amplitude of the n-th component of $\boldsymbol{\phi}$ and ϵ_n is a random phase associated with this component. The corresponding expressions for the free surface elevation is

$$\eta = \sum_{n=1}^{\infty} \frac{A_n}{2} e^{i(\mathbf{k_n}\cdot\mathbf{x} - \omega_n t + \epsilon_n)} + c.c. , \tag{4.49}$$

where $c.c.$ refers to complex conjugate.

Substituting these expressions into the second-order boundary value problem will lead to expressions for the second-order contributions to the random sea, as shown by *Sharma* and *Dean* [4.12]

$$\begin{aligned}\boldsymbol{\phi} = &\sum_{n=1}^{\infty} -\frac{ig}{2\omega_n} A_n \frac{\cosh k_n(h+z)}{\cosh k_n h} e^{i(\mathbf{k_n}\cdot\mathbf{x} - \omega_n t + \epsilon_n)} \\ &+ \sum_{i=1}^{\infty}\sum_{j=1}^{\infty} -\frac{ig^2 A_i A_j D_{ij}^{+}}{8\omega_i\omega_j(\omega_i + \omega_j)} \frac{|\mathbf{k}_i + \mathbf{k}_j|(h+z)}{\cosh|\mathbf{k}_i + \mathbf{k}_j|h} \\ &\times e^{i(\psi_i + \psi_j)} \\ &+ \sum_{i=1}^{\infty}\sum_{j=1}^{\infty} -\frac{ig^2 A_i A_j D_{ij}^{-}}{8\omega_i\omega_j(\omega_i - \omega_j)} \frac{|\mathbf{k}_i - \mathbf{k}_j|(h+z)}{\cosh|\mathbf{k}_i - \mathbf{k}_j|h} \\ &\times e^{i(\psi_i - \psi_j)} + c.c. ,\end{aligned} \tag{4.50}$$

where i and j are two arbitrary frequency components in the spectrum. The coefficients D_{ij}^{+} and D_{ij}^{-} are

$$D_{ij}^{+} = \frac{\left\{\begin{array}{c}(\sqrt{R_i} + \sqrt{R_j})\left[\sqrt{R_j}(k_i^2 - R_i^2) + \sqrt{R_i}(k_j^2 - R_j^2)\right] \\ +2(\sqrt{R_i} + \sqrt{R_j})^2(\mathbf{k}_i\cdot\mathbf{k}_j - R_i R_j)\end{array}\right\}}{(\sqrt{R_i} + \sqrt{R_j})^2 - k_{ij}^{+}\tanh k_{ij}^{+} h} , \tag{4.51}$$

$$D_{ij}^{-} = \frac{\left\{(\sqrt{R_i}-\sqrt{R_j})\left[\sqrt{R_j}(k_i^2-R_i^2)-\sqrt{R_i}(k_j^2-R_j^2)\right]\right\} \\ \left\{+2(\sqrt{R_i}-\sqrt{R_j})^2(\mathbf{k}_i\cdot\mathbf{k}_j+R_iR_j)\right\}}{(\sqrt{R_i}-\sqrt{R_j})^2-k_{ij}^{-}\tanh k_{ij}^{-}h} , \tag{4.52}$$

where

$$k_{ij}^{\pm} = |\mathbf{k}_i \pm \mathbf{k}_j| \tag{4.53}$$

$$R_n = \frac{\omega_n^2}{g} . \tag{4.54}$$

The associated expression for the free surface elevation is

$$\begin{aligned}\eta = &\sum_{n=1}^{\infty}\frac{A_n}{2}e^{i(\mathbf{k_n}\cdot\mathbf{x}-\omega_n t+\epsilon_n)} \\ &+\sum_{i=1}^{\infty}\sum_{j=1}^{\infty}\frac{1}{8}A_iA_j\left[\frac{D_{ij}^{+}-\mathbf{k}_i\cdot\mathbf{k}_j+R_iR_j}{\sqrt{R_iR_j}}+R_i+R_j\right] \\ &\times e^{i(\psi_i+\psi_j)} \\ &+\sum_{i=1}^{\infty}\sum_{j=1}^{\infty}\frac{1}{8}A_iA_j\left[\frac{D_{ij}^{-}-\mathbf{k}_i\cdot\mathbf{k}_j-R_iR_j}{\sqrt{R_iR_j}}+R_i+R_j\right] \\ &\times e^{i(\psi_i-\psi_j)} .\end{aligned} \tag{4.55}$$

The terms $\psi_i+\psi_j$ and $\psi_i-\psi_j$ denote the sum and difference interactions, respectively. Of particular importance is the difference interaction $\psi_i-\psi_j$, a much longer wave than those wave components responsible for its generation and which is considered to have a role in harbor oscillation and seiching.

The waves generated by this second-order mechanism, as mentioned above, will not grow without limit, as they do not satisfy the linear dispersion relation and, thus, are not free waves. Resonant interactions, which generate waves that do satisfy the linear dispersion relation, are a particular subset of interactions. It can be shown [4.13] that no resonant interactions appear at second order (save for one trivial set), and one must go to third order to determine these interactions. The application of multiple scale techniques to address these resonances was first performed by *Benney* [4.14], and the resulting evolution equations are quite complicated; however, the resonance conditions can be written generically as follows

$$\psi_l + \psi_m - \psi_p = \psi_n , \tag{4.56}$$

where l, m, and p are indices that represent wave components which interact with ψ_n. These quartet interaction terms have been approximated for wind wave generation models [4.15] and are a primary engine for energy transfer within the spectrum in wind wave generation.

4.5 Shallow Water Wave Theories

In contrast to deep water, there is a distinct difference in the scale of variability between horizontal and vertical motions in shallow water (small kh). The horizontal motions are scaled similarly to deep water, but the vertical motions for small kh are

$$\begin{aligned}w = \frac{\partial\boldsymbol{\phi}}{\partial z} &= \frac{gkH}{2\omega}\frac{\sinh k(z+h)}{\cosh kh}\sin(kx-\omega t) \\ &\approx \frac{gHk^2(z+h)}{\omega}\times O(1) ,\end{aligned} \tag{4.57}$$

since $\sinh k(z+h) \approx k(z+h)$ for small kh. Using the shallow water asymptote of the linear dispersion relation and rearranging the shallow water asymptote of the vertical velocity w

$$\begin{aligned}w &\approx \frac{gHk^2(z+h)}{\omega} = \frac{gak^2h}{\omega}\left(1+\frac{z}{h}\right) \\ &= \frac{a}{h}\frac{\omega}{k}kh\left(1+\frac{z}{h}\right) = \delta\mu\left(\frac{\omega}{k}\right)\left(1+\frac{z}{h}\right) .\end{aligned} \tag{4.58}$$

As is the case with ϵ in deep water, two small parameters ($\delta = a/h$ and $\mu = kh$) are evident and are used for scaling. However, in this case, the vertical motions are much smaller than the horizontal motions. The shallow water asymptote of the linear dispersion relation, in addition to the scale difference between horizontal and vertical motions, is now applied to the boundary value problem. Unlike the deep water case, the governing equation here is altered

$$\frac{\partial^2\boldsymbol{\phi}}{\partial z^2}+\mu^2\frac{\partial^2\boldsymbol{\phi}}{\partial x^2} = 0 \quad -h \le z \le \eta , \tag{4.59}$$

and the disparity between horizontal and vertical motions is clear. The bottom boundary condition remains unchanged. The dynamic free surface boundary condition becomes

$$\mu^2\left(g\eta+\frac{\partial\boldsymbol{\phi}}{\partial t}\right)+\frac{\delta}{2}\left(\mu^2\left(\frac{\partial\boldsymbol{\phi}}{\partial x}\right)^2+\left(\frac{\partial\boldsymbol{\phi}}{\partial z}\right)^2\right) = 0$$

$$\text{on } z = \eta , \tag{4.60}$$

and the kinematic free surface boundary condition becomes

$$\mu^2\left(\frac{\partial\eta}{\partial t}+\delta\frac{\partial\eta}{\partial x}\frac{\partial\boldsymbol{\phi}}{\partial x}\right)=\frac{\partial\boldsymbol{\phi}}{\partial z}\quad\text{on } z=\eta\,. \tag{4.61}$$

Rather than using Taylor series about $z=0$ to address the unknown position of the free surface (as was done for Stokes theory), a power series for the depth dependence is used. This takes advantage of the fact that vertical variation of dynamical variables is weak in shallow water

$$\boldsymbol{\phi}(x,z,t)=\sum_{n=0}^{\infty}\left(\frac{z}{h}+1\right)^n\boldsymbol{\phi}_n(x,t)\,. \tag{4.62}$$

This expression for the velocity potential $\boldsymbol{\phi}$ can further be altered to satisfy the governing equation and the bottom boundary condition. The power series can then be expressed in terms of $\boldsymbol{\phi}_0$, the velocity potential at $z=-h$

$$\boldsymbol{\phi}=\boldsymbol{\phi}_0-\frac{\mu^2}{2}\left(\frac{z}{h}+1\right)^2\frac{\partial^2\boldsymbol{\phi}_0}{\partial x^2}+\frac{\mu^4}{24}\left(\frac{z}{h}+1\right)^4\frac{\partial^4\boldsymbol{\phi}_0}{\partial x^4}+O(\mu^6)\,. \tag{4.63}$$

This is then substituted into the kinematic and dynamic free surface boundary conditions and then integrated over depth. The result is a set of mass and momentum conservation equations, which are expressed in terms of powers of μ and δ, consistent with a weakly dispersive, weakly nonlinear assumption. Retaining terms up to $O(\delta,\mu^2)$ leads to the Boussinesq equations [4.16]

$$\frac{\partial\eta}{\partial t}+\frac{\partial}{\partial x}\left([h+\eta]\,\overline{u}\right)=0 \tag{4.64}$$

$$\frac{\partial\overline{u}}{\partial t}+\overline{u}\frac{\partial\overline{u}}{\partial x}+g\frac{\partial\eta}{\partial x}-\frac{h^2}{3}\frac{\partial^3\overline{u}}{\partial^2 x\partial t}=0\,, \tag{4.65}$$

where $\overline{u}$ is a depth-averaged velocity.

4.5.1 Properties of Weakly Nonlinear Shallow Water Waves

The Boussinesq equations can be modeled numerically for general wave propagation conditions. However, they can be further transformed into a single wave equation for η. This equation is known as the Korteweg–deVries (KdV) equation

$$\frac{\partial\eta}{\partial t}+c\frac{\partial\eta}{\partial x}+\frac{3c}{2h}\eta\frac{\partial\eta}{\partial x}+\frac{ch^2}{6}\frac{\partial^3\eta}{\partial x^3}=0\,, \tag{4.66}$$

where $c=\sqrt{gh}$. Due to an ambiguity in the derivation of the KdV equation, there are actually eight formally identical forms, but the form above is generally the version used.

The KdV equation is, in fact, exactly integrable. Two general analytic solution forms are possible with the KdV equation, each representing a wave of permanent form. The first is known as a solitary wave and is a wave consisting of an isolated hump of water with no trough. This wave is often used as a proxy for a tsunami propagating away from its origin. The free surface of a solitary wave is

$$\eta(x,t)=\eta_{\max}\operatorname{sech}^2\left[\frac{\sqrt{3}}{2}\left(\frac{\eta_{\max}}{h^3}\right)^{1/2}(x-ct-x_0)\right], \tag{4.67}$$

where $\eta_{\max}$ is the (specified) maximum free surface elevation and x_0 is the location of $\eta_{\max}$. One property of the solitary wave is that the wave form becomes narrower and more peaked as $\eta_{\max}$ increases. The phase speed c of the solitary wave is

$$c=\sqrt{gh}\left(1+\frac{\eta_{\max}}{h}\right)\,. \tag{4.68}$$

Figure 4.3 shows the free surface profile of a solitary wave for different values of η_{max}. The second form is a periodic wave known as a *cnoidal* wave, so named due to its dependence on the Jacobian *cn* function. Some of the calculable properties of cnoidal waves are listed below

$$c^2=gh\left(1+\frac{H}{h}\left[-1+\frac{2}{m}-\frac{3E(m)}{mK(m)}\right]\right)\,, \tag{4.69}$$

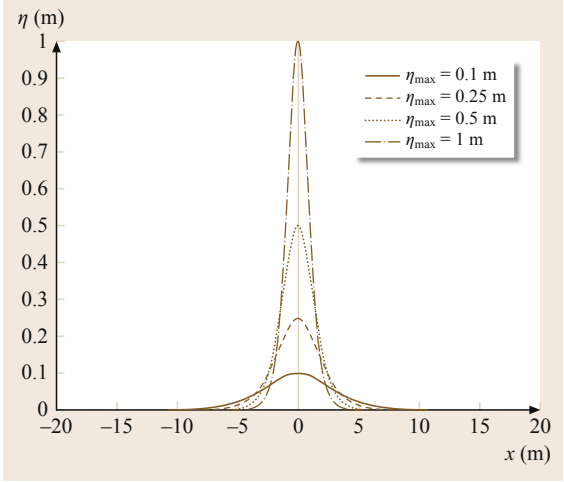

Fig. 4.3 Free surface profiles of a solitary wave with different values of $\eta_{\max}$

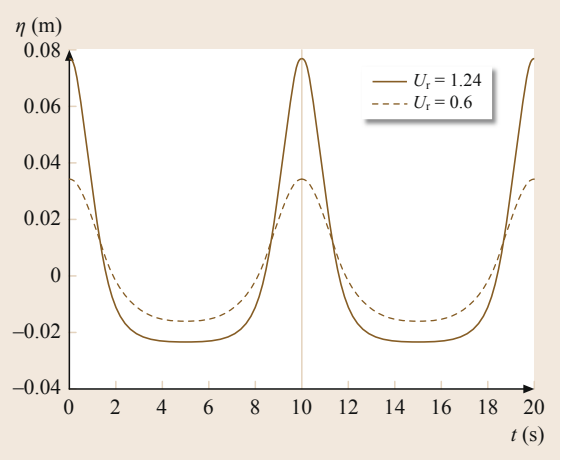

Fig. 4.4 Free surface profile of a cnoidal wave for two different values of the Ursell number U_r

$$\lambda = 4kh\left(\frac{m}{3\frac{H}{h}}\right)^2 , \tag{4.70}$$

$$T = \left(\frac{h}{g}\right)^2 \frac{4K(m)\left[\frac{h}{3H}\right]^2}{1+\frac{H}{h}\left(\frac{1}{2m}\right)\left(-m+2-3\frac{E(m)}{K(m)}\right)} , \tag{4.71}$$

$$\eta = \eta_2 + Hcn^2\left(\frac{2K(m)}{\lambda}(x-ct)\right) , \tag{4.72}$$

In these equations, $K(m)$ and $E(m)$ are the complete elliptic integrals of the first and second kind, respectively; m is a parameter, λ is the wave length, T is the wave period, and η_2 is the distance from the wave trough to the bottom at $z = -h$. The parameter m can be related to wave characteristics and determines the shape of the cnoidal wave; $m = 0$ recovers a sinusoidal wave, while $m = 1$ leads to a solitary wave. *Wiegel* [4.17] developed a straightforward procedure for calculating cnoidal wave profiles based on specified wave characteristics. Figure 4.4 shows cnoidal wave profiles for a wave with $t = 10$ *s* for two different values of the Ursell number $U_r = \delta/\mu^2$.

4.5.2 Evolution of Weakly Nonlinear Shallow Water Waves

In the context of irregular waves, this description of nearshore wave evolution can be described in terms of *wave–wave interaction*, a mechanism whereby waves of different frequencies in the spectrum can trade energy to alter the shape of the spectrum. This was mentioned earlier as a means by which wind sea transforms to long-period swell in the deep ocean. In the nearshore, the net effect of wave–wave interaction is to transfer energy from low frequencies to high ones; this accounts for changes in the spectral shape as waves evolve over sloping bathymetry; this was first described in detail by *Freilich* and *Guza* [4.18].

As with deep water waves, wave–wave interaction in shallow water is controlled by resonance between components of the wave spectrum. Unlike deep water, shallow water nonlinearity is dictated by *near*-resonant interaction among triads of waves. Given any arbitrary triad of wave components in a spectrum, the interaction triad is defined as

$$f_3 = f_2 + f_1 , \tag{4.73}$$

$$k_3 = k_2 + k_1 + O(\delta) , \tag{4.74}$$

where δ is a (small) parameter that describes the detuning away from perfect resonance. At the shallow water limit ($kh \to 0$) the parameter $\delta \to 0$, but even with finite δ significant energy transfer can take place. While the quartet interactions drive nonlinear energy transfer that occurs over spatial scales on the order of tens of kilometers, triad interactions force energy exchange, which can occur over tens of meters, drastically changing the shape and characteristics of the waves. These nonlinear interactions have been embedded into wave shoaling models, starting with *Freilich* and *Guza* [4.18], who derived a nonlinear shoaling model from the Korteweg–deVries equation, resulting in

$$\frac{\partial A_n}{\partial x} + \frac{1}{4h}\frac{\partial h}{\partial x}A_n - \frac{in^3k^3h^2}{6}A_n = \left[\sum_{l=1}^{N-1} A_l A_{n-l} + 2\sum_{l=1}^{N-n} A_l^* A_{n+l}\right] , \tag{4.75}$$

where A_n is the complex amplitude of the n-th Fourier component

$$\eta(x,y,t) = \sum_{n=1}^{N} \frac{A_n}{2} e^{i\int k_n \mathrm{d}x - \omega_n t} + c.c. , \tag{4.76}$$

and

$$nk = \frac{n\omega}{\sqrt{gh}} . \tag{4.77}$$

One limitation of this shoaling equation is the weakly dispersive assumption, which can be problematic for high frequency waves even in shallow water. This has been addressed via finite depth wave theory [4.19–22], among others.

4.6 Transformation of Waves Approaching Land

As waves approach the shoreline they undergo significant transformation in response to the arbitrarily varying bathymetry. Refraction and shoaling (as discussed above) will occur, but cannot be described by the Snell's law formulation. In addition, wave diffraction (the flow of energy along a wave crest due to high local gradients of wave height, and most often associated with waves encountering breakwaters) is also possible over bathymetric shoals.

The mild slope equation, developed by *Berkhoff* [4.23], has been used to simulate wave propagation over arbitrarily varying bathymetry

$$\nabla \cdot \left(CC_g \nabla \boldsymbol{\phi}\right) + k^2 CC_g \boldsymbol{\phi} = 0 \,, \tag{4.78}$$

where ∇ refers to differential operations in the horizontal (x, y) directions. It can be shown that the equation reduces to the Helmholtz equation for a flat bottom, and that it can also be transformed into a set of coupled equations for wave refraction by neglecting curvature terms. The equation is elliptic, which requires prespecification of the boundaries in advance. This is straightforward for enclosed harbors but challenging for open coasts, in which the location of wave breaking is unknown in advance. This has been addressed in the model's elliptic form [4.24]. However, the model has been transformed into a parabolic form [4.25], which affords a more straightforward numerical solution. *Kirby* [4.26] outlines several limitations of the parabolic form and offers some measures for ameliorating these limitations. The mild slope equation has been augmented with nonlinear interaction terms [4.20, 22, 27].

In the nearshore area, wave breaking is primarily controlled by the proximity of the bottom. The wave transformation process will force the wave to reach a limiting wave height, beyond which it cannot sustain its form. At this point the wave breaks. The breaking process and resultant generation of white water in the nearshore (the *surf zone*) is a major engine of nearshore processes (current generation, rip currents, infragravity waves, sediment transport, etc.)

The location of the initial breaking (or *incipient breaking*) of the wave demarcates the outer edge of the surf zone. It is important to identify conditions leading to incipient breaking for several reasons. For example, it is important in numerical modeling of wave propagation in the nearshore, since the wave breaking and dissipation terms are only activated within the surf zones, so it is essential to know when they need to be active.

One of the first incipient breaking criteria was developed by *McCowan* [4.28], who adapted the deep water solution of *Stokes* [4.10] to shallow water. Both studies assumed that a wave broke when the particle acceleration at the crest exceeds gravitational acceleration g, and showed that this condition resulted in an included crest angle of 120°. *McCowan* [4.28], however, also showed that, at this breaking condition

$$\frac{H_b}{h_b} = 0.78 \,, \tag{4.79}$$

or that the wave height reaches approximately 80% of the water depth at breaking. This criterion was developed using the properties of a solitary wave over a flat bottom, which would not generally fit the model of oscillatory motions in the surf zone. In an alternative treatment, *Miche* [4.29] developed a breaking criterion connected with wave steepness

$$\left(\frac{H_b}{L_b}\right) = \frac{1}{7} \tanh kh_b \,. \tag{4.80}$$

Note that this criterion approaches the maximum steepness criterion of *Stokes* [4.10] in deep water (large kh) and $H_b/h_b = 0.9$ in shallow water. A more complete development of the breaking criterion was developed by *Weggel* [4.30], who examined results from a number of laboratory experiments and determined that the bottom slope played an important role in the initiation of breaking. The resulting criterion is

$$\frac{H_b}{h_b} = b(m) - a(m)\frac{H_b}{gT^2} \,, \tag{4.81}$$

where

$$a(m) = 43.8\left(1 - e{-}19m\right) \,, \tag{4.82}$$

$$b(m) = \frac{1.56}{\left(1 + e^{-19.5m}\right)} \,. \tag{4.83}$$

This criterion reduces to (4.79) when the slope $m = 0$. Equation (4.81) is implicit for the breaking wave height H_b, so iteration is required.

Once the wave has broken, a description of the decay of the wave energy in the surf zone is needed. In this section, we discuss wave height decay mechanisms for both monochromatic and random waves. In general, the assumption of a spilling breaker is used; random wave formulations are typically determined by marrying this assumption to a probability distribution of some kind.

The equivalence between the energy decay in a spilling breaking wave and that of a hydraulic jump has been well established [4.31]. *Horikawa* and *Kuo* [4.32] conducted laboratory tests on breaking waves and determined the existence of a *stable* energy flux, which defines a state at which waves no longer break. This concept was further developed into a general description of wave evolution in the surf zone [4.33], with the hypothesis that the change in energy flux in the surf

zone would follow

$$\frac{\partial EC_g}{\partial x} = -\frac{K}{h}\left[EC_g - EC_{gs}\right] , \tag{4.84}$$

where K is a dimensionless decay coefficient, h is the still water depth, EC_g is the energy flux and the subscript s refers to the stable energy flux sought by the wave. Using shallow water wave theory and assuming that the stable wave height H_{stable} is a linear function of the water depth

$$H_{stable} = \Gamma h , \tag{4.85}$$

where Γ is a dimensionless coefficient, (4.84) can be transformed,

$$\frac{\partial\left[H^2\sqrt{h}\right]}{\partial x} = -\frac{K}{h}\left[H^2\sqrt{h} - \Gamma^2 h^{5/2}\right] . \tag{4.86}$$

Dally et al. [4.33] determined that $K = 0.15$ and $\Gamma = 0.4$ for minimum error to the data of *Horikawa* and *Kuo* [4.32]. *Dally* et al. [4.33] went on to develop analytical solutions for various bathymetric profiles, but (4.86) was the primary result.

Breaking of irregular waves in the surf zone requires a different approach than that for monochromatic waves, accommodating the random nature of waves by marrying the physics of wave breaking with probability theory. Early work by *Battjes* [4.34] and *Goda* [4.35] addressed the irregular nature of waves but did not allow for their evolution in the surf zone, constraining the statistical wave height measure to be some ratio between the wave height and the water depth.

Battjes and *Janssen* [4.36] developed a random wave breaking model based on energy flux conservation principles

$$\frac{\partial\overline{EC_g}}{\partial x} = -D , \tag{4.87}$$

where the overbar refers to averaged quantities and D is a dissipation rate. *Battjes* and *Janssen* [4.36] developed this dissipation rate from that of a dissipating bore, and introduced random wave heights by using the assumption that the heights of unbroken nearshore waves follow a Rayleigh distribution [4.37] for a range of heights that vary between zero and the maximum realizable wave height H_{max} at a particular water depth. The resulting dissipation rate D is

$$D = \frac{\alpha}{4} Q_b \overline{f} \rho g H_{max}^2 , \tag{4.88}$$

where H_{max} is the maximum wave height, Q_b is the percentage of breaking waves in a population of waves, $\overline{f}$ is an average frequency, and the coefficient α is of order 1. The maximum wave height is based on the *Miche* [4.29] criterion for maximum wave height, with some modification for the random nature of waves. This was then combined with the Rayleigh distribution for nearshore wave heights and further manipulated to lead to an expression for the fraction of breaking or broken waves Q_b

$$\frac{1 - Q_b}{\ln Q_b} = -\left(\frac{H_{rms}}{H_{max}}\right)^2 , \tag{4.89}$$

which is transcendental in Q_b. The model thus uses the offshore estimate of H_{rms} (from a measurement or a model) to calculate H_{max}, then Q_b from (4.89), and finally D from (4.88). With this estimate of the dissipation rate, (4.87) is then used to calculate the energy (and H_{rms}) at the new position.

Thornton and *Guza* [4.38] commented that the formulation of *Battjes* and *Janssen* [4.36] was, in effect, the implementation of a sharp cutoff value of the probability distribution of wave heights at H_{max}. They argue that waves in a group can momentarily exceed H_{max}, so a more gradual cutoff of the probability distribution near the maximum wave height is required. They then developed two weightings for this region of the probability distribution, either of which would allow wave heights above the theoretical maximum to occur. Using the same dissipative bore paradigm as *Battjes* and *Janssen* [4.36] but with different parameters, using the weightings, and integrating over the Rayleigh probability distribution, they determined two different dissipation rates for random waves. The first,

$$D = \frac{3\sqrt{\pi}}{16}\rho g \frac{B^3\overline{f}}{\gamma^4 h^5} H_{rms}^7 , \tag{4.90}$$

was less accurate when compared to data but leads to an analytical solution, while the second,

$$D = \frac{3\sqrt{\pi}}{16}\rho g B^3 \overline{f} \frac{H_{rms}^5}{\gamma^2 h^3}\left[1 - \frac{1}{\left(1 + \left(\frac{H_{rms}}{\gamma h}\right)^2\right)^{5/2}}\right] , \tag{4.91}$$

compared relatively well to data. The parameter B is nominally defined as the proportion of the front face of a breaking wave covered in foam, while γ is the ratio of the wave height to water depth in the surf zone; both are generally calibrated to data. *Thornton* and *Guza* [4.38] have shown that $\gamma = 0.42$ and $1.3 \le B \le 1.7$ work well for field data.

Both mechanisms have been used as a basis for the incorporation of random wave breaking into nonlinear phase-resolving models [4.20, 39]. The model of *Battjes* and *Janssen* [4.36] has been further extended for steep slopes [4.40], following work by *Baldock* et al. [4.41].

There is ample evidence for the existence of very long period of motion in the nearshore. These motions are generally thought to be largely the result of time variation of wave heights and breaking locations [4.42], though contributions from nonlinear wave–wave interactions [4.43] (see also *Bowen* and *Guza* [4.44]) may also be responsible. These long waves (often termed *infragravity* waves) have periods on the order of minutes and play a significant role in the evolution of the beach face.

The basic equations governing these long wave motions can be derived from the uniform depth equations of motion; the details can be found in [4.45]. The result can be expressed as an inhomogeneous wave equation

$$\frac{\partial^2\overline{\eta}}{\partial t^2} - \frac{\partial}{\partial x}\left(gh_O\frac{\partial\overline{\eta}}{\partial x}\right) - \frac{\partial}{\partial y}\left(gh_O\frac{\partial\overline{\eta}}{\partial y}\right) = F\,, \quad (4.92)$$

where h_O is a representative water depth and $\overline{\eta}$ is a mean (wave-averaged) free surface elevation. The term F represents forcing of the long wave motion.

In many cases [4.46], the long wave motion in the nearshore results from the transformation of long wave energy from offshore; the long wave propagates as a free wave. In this case, $F = 0$ in (4.92). The resulting motion in the nearshore is called an *edge wave*. The mean free surface elevation is assumed to have a longshore periodicity

$$\overline{\eta} = A(x)e^{i(k_y y \pm \omega t)}\,, \quad (4.93)$$

where $k_y = k\sin\theta$, or the longshore component of the wave number; the wave approach direction θ is assumed to be from shore normal. Substituting (4.93) into (4.92), and further assuming a plane beach, leads to a solution for $A(x)$ [4.47]

$$A(x) = a_n e^{-k_y x}L_n(2k_y x)\,, \quad (4.94)$$

where the subscript n denotes a mode of the solution (matching the number of zero crossings of the cross-shore structure of the edge wave) with amplitude a_n. The cross-shore structure is given by $L_n(2k_y x)$, which is the Laguerre polynomial of order n. The associated dispersion relation for this motion is

$$\omega^2 = gk_y\sin\left[(2n+1)\beta\right]\,, \quad (4.95)$$

where β is the angle of the beach from horizontal. Since there is no dissipation, the edge wave will fully reflect from the shoreline. For $n = 0$, all edge waves will propagate in the longshore direction, with crests perpendicular to the shoreline. For $n > 0$, however, the edge wave is affected by refraction; the wave reflects seaward from the shoreline, refracts to the point where the crests are perpendicular to the shoreline, then continues refracting back toward the shoreline. Such an edge wave is said to be *trapped*. On the other hand, a long wave which is *not* refracted back toward shore is said to be *leaky*. The phenomenon of *surf beat* [4.48, 49] is considered a leaky mode.

The discussion of edge waves in the previous section is useful as an introduction to nearshore long waves. However, because the motion is free, these long wave frequencies must be present at reasonable energy levels in the incident wave spectrum. The more significant source of long wave energy in the nearshore and surf zones comes from forced motion [4.46]. In this case, the forcing term F in (4.92) would be nonzero. If we dictate that the forcing is (as for nearshore circulation) dependent on the gradients of radiation stress [4.50], then the term F becomes

$$F = \frac{1}{\rho}\frac{\partial^2 S_{xx}}{\partial x^2}\,, \quad (4.96)$$

where the analysis is limited to processes in the cross-shore direction only (longshore derivatives are zero in (4.92)). In a wave group, the changes in radiation stress are assumed to be due to the spatial variations of the wave heights within the group. Using this assumption and limiting the domain to a constant water depth h_O gives the following solution for the mean sea surface

$$\overline{\eta} = -\frac{S_{xx}(x,t)}{\rho(gh_O - c_g)}\,, \quad (4.97)$$

where it can be seen that the mean sea surface is in antiphase with the gradient of radiation stress. Besides the limitation to constant depth, this solution is problematic in that $\overline{\eta}$ becomes quite large as the group velocity of the short waves in the group begins to approach the shallow water asymptote.

Later approaches sought to remedy these issues and move the area of interest closer to the surf zone. *Symonds* et al. [4.42] represented the wave group as a prescribed wave height variation about a mean amplitude and propagating over a sloping bottom, then used a constant breaking height-to-depth ratio *breaking index* inside the surf zone. The varying wave height led to a moving breakpoint, which served as a varying boundary condition for the generation of the long wave. The assumption of a constant breaking index was used to constrain the wave height in the surf zone, but destroyed any remaining group structure therein, which was later shown to be at least partially incorrect [4.51]. *Foda* and *Mei* [4.52] and *Schäffer* and *Svendsen* [4.53] perused an alternative formulation, in which the breakpoint was fixed but allowed for the group structure to remain in the surf zone.

The growth of the infragravity waves after this initial generation must now be considered. *Elgar*

et al. [4.54] showed that the infragravity wave energy tends to be a function of $h^{1.1}$, an almost linear dependence. However, coupling (4.97) with Green's Law shoaling yielded a growth rate closer to h^{-5}. The discrepancy is due to how the wave environment in the surf zone is treated. *Van Dongeren* and *Svendsen* [4.55], using a quasi-3-D (three-dimensional) nearshore circulation model, showed that the growth rate of infragravity waves can be dictated by manipulating the phase difference between the bound wave (locked with the wave group) and a free wave in the surf zone. Later, *Janssen* et al. [4.56] developed an analytical solution for the phase shift, leading to growth rates more consistent with measurements [4.57].

Oltman-Shay et al. [4.58], examining wave-like structures in nearshore current data taken at Duck, NC (USA), found that these structures did not correspond to any known wave theory. *Bowen* and *Holman* [4.59] applied stability theory to the equations governing nearshore circulation (with several simplifying assumptions) and determined that the most unstable modes had frequencies that were in the range of those observed in [4.58]. These instabilities were termed *shear waves* since they seemed to be caused by the shear instabilities of the longshore current. These motions only appeared when the longshore current was present and sufficiently energetic. The speed of these waves was independent of their frequency (a nondispersive phenomenon) and their signature in frequency longshore wave number space is both distinct and distinctly different from gravity wave phenomena.

Since the original papers there have been numerous studies on these shear waves. *Reniers* et al. [4.60] recreated these waves in the laboratory. Analytical means of studying the growth of these phenomena were advanced by *Dodd* and *Falques* [4.61], *Shrira* et al. [4.62], and *Feddersen* [4.63], among others. Additionally, the modeling of shear waves became a motivating factor for the development and application of numerical models of nearshore circulation ([4.64, 65], among others).

4.7 Computational Method for Fully Nonlinear Waves

With the development of powerful computers, numerical methods have been developed to tackle nonlinear wave problems and problems involving arbitrary body boundaries. Boundary integral methods are found to be more efficient for solving wave problems formulated using the potential flow theory, in particular to handle steep and overturning waves and complex body boundary shapes. For linear problems, boundary integral methods based on the free surface Green's function have been developed for analysis in both the frequency and time domains. Frequency domain analysis using a simple Rankine source has also been used to studying linear wave–body interaction problems in the frequency domain. An excellent review on numerical methods for free surface flows is given in [4.66].

Longuet-Higgins and *Cokelet* [4.4] developed a boundary integral method to solve the fully nonlinear inviscid wave motion problem. The method involves solution of Green's theorem, which is based on the Eulerian description of flow and the nonlinear free surface boundary conditions in the Lagrangian form; the method is, therefore, considered to be based on the mixed Eulerian–Lagrangian (MEL) formulation. To illustrate the method, let us consider a wave–body interaction problem such as that depicted in Fig. 4.1. Let the lateral extent of the domain be truncated by an open boundary Σ. Let us say that the flow has been started from rest with the initial condition being $\phi = 0$ and $\eta = 0$ at time $t = 0$. Since Σ is not a physical boundary, it has to be modeled so that waves incident on it may pass through without any reflection. There are several ways to achieve that approximately, as through use of nonlinear wave equations, free surface damping etc. Here let us consider a simple model by which it is assumed that $\phi = 0$ on Σ during the duration of flow simulation; in other words, simulation will be carried out only until the radiating waves reach the vicinity of the open boundary Σ.

Per Green's theorem,

$$2\pi\phi(P) + \int_{\partial\Omega} \phi \frac{\partial}{\partial n}\frac{1}{r_{PQ}} \mathrm{d}\partial\Omega - \int_{\partial\Omega} \frac{1}{r_{PQ}}\frac{\partial\phi}{\partial n}\mathrm{d}\partial\Omega = 0\,, \tag{4.98}$$

where $\partial\Omega$ is the union of all boundaries; i. e., $\partial\Omega = B + S_\mathrm{B} + \mathcal{F} + \Sigma$. Here Green's function $1/r_{PQ}$ corresponds to the potential at P due to the point source at Q. On B and S_B the normal velocity $\partial\phi/\partial n$ is known based on the no-flux condition, while ϕ is not known. On the open boundary, ϕ is known, here set to be zero, while $\partial\phi/\partial n$ is not known. On the free surface, one can time integrate the fully nonlinear free surface conditions at each time step to determine the free surface deformation and the velocity potential on the free surface; in other words, time integrate the dynamic condition

$$\frac{D\phi}{Dt} = \frac{1}{2}|\nabla\phi|^2 - \mathrm{g}Y\,,$$

to advance ϕ from discrete time n to $n+1$ and time integrate the free surface (material surface) kinematic

condition

$$\frac{D\boldsymbol{X}}{Dt} = \nabla\boldsymbol{\phi}\ ,$$

to advance position of free surface nodes $\boldsymbol{X} = (X, Y, Z)$ from discrete time n to $n+1$. Algorithms such as the fourth-order Runge–Kutta and Adams–Bashforth schemes [4.67, 68] may be used for the time integration. Thus, knowing $\boldsymbol{\phi}$ on the free surface, one may rewrite the above Green's theorem with known terms on the right-hand side and unknown terms on the left-hand side

$$\begin{aligned}
&2\pi\boldsymbol{\phi}(P \in B + S_B) \\
&+ \int\limits_{B+S_B} \boldsymbol{\phi}\frac{\partial}{\partial n}\frac{1}{r_{PQ}}\mathrm{d}\partial\Omega - \int\limits_{\Sigma+\mathcal{F}} \frac{1}{r_{PQ}}\frac{\partial\boldsymbol{\phi}}{\partial n}\mathrm{d}\partial\Omega \\
&= -2\pi\boldsymbol{\phi}(P \in \mathcal{F} + \Sigma) \\
&\quad - \int\limits_{\mathcal{F}+\Sigma} \boldsymbol{\phi}\frac{\partial}{\partial n}\frac{1}{r_{PQ}}\mathrm{d}\partial\Omega + \int\limits_{B+S_B} \frac{1}{r_{PQ}}\frac{\partial\boldsymbol{\phi}}{\partial n}\mathrm{d}\partial\Omega\ . \qquad (4.99)
\end{aligned}$$

The above integral equation is discretized and the resulting algebraic (matrix) equation solved either directly or iteratively for $\boldsymbol{\phi}$ on solid boundaries B and S_B, and for $\partial\boldsymbol{\phi}/\partial n$ on the free surface $\mathcal{F}$ and open boundary Σ. Upon determining $\boldsymbol{\phi}$ on the body, one can use the Euler integral (unsteady Bernoulli's equation) to determine pressure and through integration of pressure the hydrodynamic force on the body. The solution is thus advanced in time.

The mixed Eulerian–Lagrangian formulation has become a standard approach for solving fully nonlinear inviscid wave and wave–body interaction problems and it has been adopted in field discretization methods such as the finite difference method. Works on nonlinear wave and wave–body interaction problems based on the MEL formulation include those by *Vinje* and *Brevig* [4.69], *Grosenbaugh* and *Yeung* [4.67], *Dommermuth* et al. [4.68], *Saout* and *Ananthakrishnan* [4.70], *Ananthakrishnan* [4.71] and Xue et al. [4.72].

4.8 Wave Forces on Fixed and Floating Structures

In this section, the methods to determine the wave exciting force (which consists of incident and body-diffracted wave forces) on a body, and in the case of a freely floating body the additional wave radiation force due to the body motion generated waves are presented. Both theoretical and numerical methods to determine the wave forces will be discussed. We shall take the mean forward of the bodies to be zero here. One can find the nonzero forward speed cases in the literature on ship hydrodynamics and naval architecture. Empirical and exact methods to determine the viscous drag force is also discussed. Particular emphasis is given to parameters that govern ratios of various wave component and viscous drag forces.

4.8.1 Incident Wave Force: Froude–Krylov Force

Let us consider a body (submerged or floating) in a wave field as illustrated in Fig. 4.1. Let the incident wave be of small amplitude and be propagating in the positive x direction with elevation and potential given by

$$\eta^{\mathrm{i}} = \frac{H^{\mathrm{i}}}{2}\cos(kx - \omega t)\ ,$$

$$\boldsymbol{\phi}^{\mathrm{i}} = \frac{H^{\mathrm{i}}}{2}\frac{\cosh k(z+h)}{\cosh kh}\sin(kx - \omega t)\ ,$$

where the superscript i denotes incident wave. Using the Euler integral, one can find the dynamic pressure of the incident wave as

$$p^{\mathrm{i}} = -\rho\frac{\partial\boldsymbol{\phi}^{\mathrm{i}}}{\partial t} = \rho g\frac{H^{\mathrm{i}}}{2}\frac{\cosh k(z+h)}{\cosh kh}\cos(kx - \omega t)\ .$$

By integrating the incident wave pressure about the body surface (mean surface if the body is undergoing oscillation) one can determine the incident wave force, which is also known as the Froude–Krylov force, $\boldsymbol{F}^{\mathrm{i}}$

$$\begin{aligned}
\boldsymbol{F}^{\mathrm{i}} &= \int\limits_{S_o} p^{\mathrm{i}}\mathrm{d}S_o \\
&= \int\limits_{S_o} \rho g\frac{H^{\mathrm{i}}}{2}\frac{\cosh k(z+h)}{\cosh kh}\hat{n}\cos(kx - \omega t)\,\mathrm{d}S_o\ ,
\end{aligned}$$

where S_o denotes the body surface and $\hat{n}$ the unit normal vector into the body. Using the Gauss theorem one may write the above as a volume integral

$$\boldsymbol{F}^{\mathrm{i}} = \int\limits_{S_o} p^{\mathrm{i}}\hat{n}\mathrm{d}S_o = -\int\limits_{\forall_o} \nabla p^{\mathrm{i}}\mathrm{d}\forall_o\ ,$$

where $\forall_o$ denotes the volume occupied by the body. In the component form, the incident wave forces are then

$$\begin{aligned}
F_x^{\mathrm{i}} &= \rho g k\frac{H^{\mathrm{i}}}{2}\frac{1}{\cosh kh} \\
&\quad \times \int\limits_{\forall_o} \cosh k(z+h)\sin(kx - \omega t)\mathrm{d}\forall_o\ ,
\end{aligned}$$

and

$$F_z^{\mathrm{i}} = -\rho g k \frac{H^{\mathrm{i}}}{2} \frac{1}{\cosh kh} \times \int_{\forall_{\mathrm{o}}} \sinh k(z+h) \cos(kx - \omega t) \mathrm{d}\forall_{\mathrm{o}} .$$

If the body is really small, or more precisely spans small distances along x and z compared to the incident wave length, then the above integral may be further approximated by replacing x and z in the integrals by the x and z coordinates of the centroid. The Froude–Krylov force will then simply be

$$F_x^{\mathrm{i}} = \rho g k \frac{H^{\mathrm{i}}}{2} \frac{\cosh k(\bar{z}+h)}{\cosh kh} \sin(k\bar{x} - \omega t) \ \forall_{\mathrm{o}} ,$$

and

$$F_z^{\mathrm{i}} = -\rho g k \frac{H^{\mathrm{i}}}{2} \frac{\sinh k(\bar{z}+h)}{\cosh kh} \cos(k\bar{x} - \omega t) \ \forall_{\mathrm{o}} ,$$

where $(\bar{x}, \bar{z})$ denote the coordinates of the centroid of the body (submerged part of the body if the body were floating). It is thus a straightforward calculation to determine the small amplitude incident wave force, in particular if the body size is small compared to the incident wave length.

From the above integrals, one can also estimate the order of magnitude of the incident wave force. For a near surface body, the incident wave force is of the order of magnitude

$$|\boldsymbol{F}^{\mathrm{i}}| \equiv F^{\mathrm{i}} = O(\rho g \forall_{\mathrm{o}} k \frac{H^{\mathrm{i}}}{2}) = \Delta O(k \frac{H^{\mathrm{i}}}{2}) ,$$

where Δ denotes the weight (displacement) of the body.

Note that $kH^{\mathrm{i}}/2$ denotes the slope of the incident wave. In other words, the Froude–Krylov force of the order of body weight times the wave slope.

4.8.2 Morison Force on a Stationary Body

The incident wave force given by the Froude–Krylov force does not account for the viscous drag force, which could be significant even if the body size is small compared to the incident wave length. Computing the viscous drag force exactly would require solving the incompressible Navier–Stokes equation with free surface conditions, which is a formidable task. *Morison* et al. [4.73] proposed an empirical method to determine the wave force on a body including the drag force. Decomposing the hydrodynamic force into inertia and drag components, which is exact for force on a submerged body without a free surface, Morison proposed to determine the wave force as

$$F = F_{\mathrm{inertia}} + F_{\mathrm{drag}} .$$

In terms of inertia and drag coefficients,

$$F = C_{\mathrm{I}} \rho \dot{u} \forall + C_{\mathrm{d}} \frac{\rho}{2} u|u| A_{\mathrm{p}} ,$$

where F denotes the x component of the force, u the x component of fluid velocity, $\dot{u}$ the x component of fluid acceleration, $\forall$ the displaced volume of the body, and A_{p} the projected area of the body normal to the x-axis. The inertia and drag coefficients C_{i} and C_{d} are empirically obtained; scaled with respect to volume and projected area, they are both $O(1)$. The above is referred to as the Morison equation for the wave force on a body [4.8]. In the Morison equation method the fluid velocity and acceleration are determined using wave theories. As per linear Airy wave theory, as seen in an earlier section, the amplitudes of u and $\bar{u}$ are given by

$$|u| = \frac{H^{\mathrm{i}}}{2} \frac{gk}{\omega} \frac{\cosh k(z+h}{\cosh kh} ,$$
$$|\dot{u}| = \frac{H^{\mathrm{i}}}{2} gk \frac{\cosh k(z+h}{\cosh kh} .$$

The above Morison equation method thus provides a practical method to determine the viscous incident wave force on a body. The decomposition also allows one to determine the relative significance of the inertia and drag components of the incident wave force. For a body in a wave under wave influence (i. e., $kz \approx 0$)

$$\frac{\text{Drag}}{\text{Inertia}} = \frac{C_{\mathrm{d}} \rho u|u| A_{\mathrm{p}}/2}{C_{\mathrm{I}} \rho \dot{u} \forall} = O\left(\frac{H^{i2} g^2 k^2 D^2}{\omega^2 H^{\mathrm{i}} g k D^3}\right)$$
(here D denotes body length)
$$= O\left(\frac{H^{\mathrm{i}} g k}{\omega^2 D}\right) = O\left(\frac{H^{\mathrm{i}}}{D} \frac{1}{\tanh kh}\right)$$
(using the dispersion relation) .

From the above, it is clear that the drag force is more significant for a large wave height to body length ratio and/or in shallow water (i. e., small kh) [4.8]. Using wave kinematics, one can easily establish that in the case of deep water waves, the above ratio is related to the Keulegan–Carpenter number KC of oscillating flows [4.74]

$$KC \equiv \frac{UT}{D} = \frac{\left(\frac{H^{\mathrm{i}}}{2\,\omega}\right)\left(\frac{2\pi}{\omega}\right)}{D} = \frac{H^{\mathrm{i}}}{D} .$$

From the above discussion, the following points are worth recapitulating:

- The ratio of drag force to inertia force depends on (i) the wave height to body diameter ratio and (ii) wave length to water depth ratio.
- In the case of small wave height to body diameter ratio H^{i}/D in deep water waves (i. e., tanh kh = 1), the Morison force will be equal to the Froude–Krylov force for appropriate value of C_i.
- When using the Morison equation method for wave force on a moving body, the velocity and accelerations are taken to be relative to the body motion.

If the body dimension is large compared to wave height and not small compared to the incident wave length, then the drag force will not be important, but the Morison equation cannot be used to determine the inertial force because the scattering (diffraction) of waves by the body will become significant. One can use the potential flow theory to solve the diffraction problem (as done in [4.75] for a vertical cylinder) and also determine the wave diffraction force. The wave exciting force will then be the sum of the Froude–Krylov and the diffraction wave forces. The diffraction wave problem pertaining to linear wave–body interaction is discussed in the next section.

4.8.3 Wave Diffraction over a Body

Let the body shown in Fig. 4.1 be stationary. The mere presence of the body will cause the incident waves to scatter. For small amplitude waves, governed by linearized free surface conditions, one may solve the diffraction problem separately and determine the total potential as

$$\boldsymbol{\phi} = \boldsymbol{\phi}^{\mathrm{i}} + \boldsymbol{\phi}^{\mathrm{d}} ,$$

where the superscripts i and d denote incidence and diffraction, respectively. The solution of the incident wave potential is simply that of a free periodic wave as presented in Sect. 3.2. The diffraction potential is governed by the following set of equations

$$\begin{aligned}
\nabla^2\boldsymbol{\phi}^{\mathrm{d}} &= 0 , \\
\frac{\partial\boldsymbol{\phi}^{\mathrm{d}}}{\partial z} &= 0, \text{ on the sea bottom } z = -h , \\
\frac{\partial\boldsymbol{\phi}^{\mathrm{d}}}{\partial n} &= -\frac{\partial\boldsymbol{\phi}^{\mathrm{i}}}{\partial n} \text{ on the body surface } S_B , \\
\frac{\partial^2\boldsymbol{\phi}^{\mathrm{d}}}{\partial t^2} + \mathrm{g}\frac{\partial\boldsymbol{\phi}^{\mathrm{d}}}{\partial z} &= 0, \text{ on the mean free surface } z = 0 .
\end{aligned}$$

Moreover, in the far field, the diffraction potential must satisfy the Sommerfeld radiation condition [4.9]

$$\sqrt{R}\left(-i\omega\boldsymbol{\phi}^{\mathrm{d}} + C\frac{\partial\boldsymbol{\phi}^{\mathrm{d}}}{\partial R}\right) = 0, \text{ as } R \to \infty ,$$

where $R = \sqrt{x^2 + y^2}$, which denotes the radial distance from the body and C the wave phase speed. The above diffraction problem was solved by *McCamy* and *Fuchs* for the case of a vertical circular cylinder [4.75]. The x component wave exciting force with diffraction is given by

$$F_{\mathrm{x}} = \frac{\rho \mathrm{g}\frac{H}{2}D^2\tanh(kh)}{k^2R^2H_1^{(2)'}(kR)} ,$$

where $H_1^{(2)}$ denotes the Hankel function of the second kind and order 1 and $R = D/2$ the radius of the cylinder.

In the case of small H/D and not so small L/D, as in the case of waves incident on a supertanker or a large gravity platform, the diffraction force will be more significant than the drag force. On the other hand, drag force will be the predominant part of the wave exciting force for a mooring cable (small diameter) in a similar sea.

4.8.4 Wave Radiation Force on an Oscillating Body

In the case of a compliant or freely floating body, the body will undergo oscillatory motion when subject to the wave exciting force. The force due to waves caused by body motion is referred to as the wave radiation force [4.9]. Now let the body considered in Fig. 4.1 undergo rigid body motion such that the normal velocity of the body may be written as

$$\begin{aligned}
V_{\mathrm{n}} &= \boldsymbol{U}\cdot\hat{n} + (\boldsymbol{\Omega}\times\boldsymbol{r})\cdot\hat{n} \\
&= \boldsymbol{U}\cdot\hat{n} + \boldsymbol{\Omega}\cdot(\boldsymbol{r}\times\hat{n}) \\
&= \sum_{i=1}^{i=6} U_i n_i ,
\end{aligned}$$

where $\hat{n}$ denotes the unit normal vector on the body surface and r the position vector from the axis of rotation through the center of gravity. Moreover, $U_i = U_1, U_2, U_3, \Omega_1, \Omega_2, \Omega_3$ and $n_i = n_1, n_2, n_3, (\boldsymbol{r}\times\hat{n})_1, (\boldsymbol{r}\times\hat{n})_2, (\boldsymbol{r}\times\hat{n})_3$ for $i = 1, 2, 3, 4, 5, 6$, respectively, corresponding to the sixth degree of freedom rigid body motion. For the linear small amplitude body and wave motion problem, the radiation wave potential can be decomposed as per Kirchoff modal decomposition [4.9]

and written as

$$\Phi^{\mathrm{r}} = \sum_{j=1}^{j=6} A_j \boldsymbol{\phi}_j^{\mathrm{r}}\, e^{-i\omega t}\,,$$

where Φ^{r} denotes the total wave radiation potential and $\boldsymbol{\phi}_i^{\mathrm{r}}$ the i-th mode of radiation potential per unit amplitude of body motion. The equations governing the unit radiation potentials are given by [4.9]

$$\begin{aligned}
\nabla^2 \boldsymbol{\phi}_j^{\mathrm{r}} &= 0\,,\\
\frac{\partial \boldsymbol{\phi}_j^{\mathrm{r}}}{\partial z} &= 0, \text{ on the sea bottom } z = -h\,,\\
\frac{\partial \boldsymbol{\phi}_j^{\mathrm{r}}}{\partial n} &= -i\omega n_j \\
&\quad \text{on the equilibrium body surface } S_{\mathrm{Bo}}\,,\\
-\omega^2 \boldsymbol{\phi}_j^{\mathrm{r}} + \mathrm{g}\frac{\partial \boldsymbol{\phi}_j^{\mathrm{r}}}{\partial z} &= 0, \,, \\
&\quad \text{on the mean free surface } z = 0\,.
\end{aligned}$$

At infinity, the radiation potential must satisfy the Sommerfeld radiation condition

$$\sqrt{R}\left(-i\omega \boldsymbol{\phi}_j^{\mathrm{r}} + C\frac{\partial \boldsymbol{\phi}_j^{\mathrm{r}}}{\partial R}\right) = 0, \text{ as } R \to \infty\,,$$

where $R = \sqrt{x^2 = y^2}$, which denotes the radial distance from the body and C the phase speed of the radiating waves (which, for example, for the deep water wave case is g/ω). Upon solving the above radiation problem, for example by using the simple source distribution method originated by *Yeung* [4.66], one can determine the complex hydrodynamic coefficient

$$f_{ij} = \rho \int_{S_{\mathrm{Bo}}} \boldsymbol{\phi}_i^{\mathrm{r}} n_j \mathrm{d}S_{\mathrm{Bo}}\,,$$

which can be decomposed into components that are proportional to body acceleration (known as the added mass force) and to velocity (known as the wave damping force)

$$f_{ij} = -\omega^2 \mu_{ij} - i\omega\lambda_{ij}\,,$$

where μ_{ij} denotes the added mass force coefficient and λ_{ij} the wave damping force coefficient, both for force/moment along direction i for the j-th mode of motion. Using Green's identity one can establish that the coefficients are symmetric: $f_{ij} = f_{ji}$. For bodies with symmetry one can show that wave damping and wave excitation forces can be related using the Haskind relation [4.9]. The linear wave–body interaction theory is thus quite useful from a practical viewpoint to determine the wave forces. The theory is also rich in classical mathematics. Thus both theoreticians and practical engineers are attracted to the subject. The reader may refer to classical texts such as those by *Wehausen* and *Laitone* [4.7], *Newman* [4.9], and *Mei* [4.76] for detailed accounts of formulation and analysis of wave–body interactions.

In the case of a linear wave body interaction problem involving freely floating bodies, one then has to solve rigid body dynamics problem to determine the body response to wave forces consisting of incident, diffraction, and radiation wave force. In the case of the fully nonlinear wave–body interaction problem, both the hydrodynamic and body dynamic problems have to solved simultaneously, as each affect the other through the boundary conditions of hydrodynamic problems and through hydrodynamic force and moment of the body dynamics problem. The hydrodynamic problem may be solved using the mixed Eulerian–Lagrangian method of *Longuet-Higgins* and *Cokelet* [4.4] discussed earlier. Between the linear and fully nonlinear wave–body interaction theories, there are also weakly nonlinear theories developed for wave forces, as for example in [4.77], which are not discussed here. As the fully nonlinear wave theories are computationally intensive, linear and weakly nonlinear theories remain useful for engineering solutions to problems involving wave and body motions.

4.9 Concluding Remarks

The fundamentals of the mechanics of ocean wave theory and wave–body interactions were presented in this chapter. It began with an overview of linear wave theory, including the assumptions and limitations inherent in its use. Weakly nonlinear deep and shallow water wave theories were then outlined, including both permanent form waves (classical *Stokes* and cnoidal wave theories), followed by a discussion of wave spectral evolution and nonlinear wave–wave interactions. The transformation of waves over arbitrarily varying bathymetry was then detailed, touching on the mild slope equation for water wave propagation, nearshore wave breaking, infragravity waves, and waves caused by instabilities of nearshore circulation. Computational

methods for calculating fully nonlinear waves and the resultant forces on bodies were discussed. The interaction of waves with a submerged or floating body was also considered, including discussions of the Froude–Krylov force of the incident wave and the Morison equation method for determining the inertia and drag-components of the wave exciting force.

Related topics such as wind wave generation, sea spectra, and wave energy conversion are discussed in other chapters of the Handbook.

References

4.1 A.D.D. Craik: The origins of water wave theory, Annu. Rev. Fluid Mech. **36**, 1–28 (2004)
4.2 J.H. Michell: The wave-resistance of a ship, Philos. Mag. **45**(5), 106–123 (1898)
4.3 E.O. Tuck: *Wave resistance of thin ships and catamarans*, Tech. Rep., Vol. T8701 (University of Adelaide, Adelaide 1987)
4.4 M.S. Longuet-Higgins, E.D. Cokelet: The deformation of steep surface waves on water: I. A numerical method of computation, Proc. R. Soc. L. A **350**, 1–26 (1976)
4.5 H. Lamb: *Hydrodynamics* (Dover, Mineola 1945)
4.6 J.J. Stoker: *Water Waves – The Mathematical Theory with Applications* (Wiley, New York 1958)
4.7 J.V. Wehausen, E.V. Laitone: Surface waves. In: *Fluid Dynamics, Encyclopedia fo Physics*, Vol. 3, ed. by C. Trusdell (Springer, Berlin, Heidlberg 1960)
4.8 R.G. Dean, R.A. Dalrymple: *Water Wave Mechanics for Engineers and Scientists*, Advanced Series on Ocean Engeneering, Vol. 2 (World Scientific, Singapure 1991)
4.9 J.N. Newman: *Marine Hydrodynamics* (MIT Press, Cambridge 1977)
4.10 G.G. Stokes: On the theory of oscillatory waves, Trans. Camb. Philos. Soc. **8**, 441–455 (1847)
4.11 V.E. Zakharov: Stability of periodic waves of finite amplitude on the surface of a deep fluid, J. Appl. Mech. Tech. Phys. **9**, 190–194 (1968)
4.12 J.N. Sharma, R.G. Dean: Second order directional seas and associated wave forces, Soc. Petroleum Eng. J. **21**, 129–140 (1981)
4.13 O.M. Phillips: *The Dynamics of the Upper Ocean* (Cambridge Univ. Press, Cambridge 1980)
4.14 D.J. Benney: Nonlinear gravity wave interactions, J. Fluid Mech. **14**, 577–584 (1962)
4.15 S. Hasselmann, K. Hasselmann: Computations and parameterizations of the nonlinear energy transfer in a gravity-wave spectrum. Part 1: A new method for efficient computations of the exact nonlinear transfer integral, J. Phys. Oceanogr. **15**, 1369–1377 (1985)
4.16 D.H. Peregrine: Long waves on a beach, J. Fluid Mech. **27**, 815–827 (1967)
4.17 R.L. Wiegel: A presentation of cnoidal wave theory for practical application, J. Fluid Mech. **7**, 273–286 (1960)
4.18 M.H. Freilich, R.T. Guza: Nonlinear effects on shoaling surface gravity waves, Philos. Trans. R. Soc. Lond. A **311**, 1–41 (1984)
4.19 Y. Agnon, A. Sheremet, J. Gonsalves, M. Stiassnie: Nonlinear evolution of a unidirectional shoaling wave field, Coast. Eng. **20**, 29–58 (1993)
4.20 J.M. Kaihatu, J.T. Kirby: Nonlinear transformation of waves in finite water depth, Phys. Fluids **7**, 1903–1914 (1995)
4.21 H. Bredmose, Y. Agnon, P.A. Madsen: Wave transformation models with exact second order transfer, Eur. J. Mech. B/Fluids **24**, 659–682 (2005)
4.22 T.T. Janssen, T.H.C. Herbers, J.A. Battjes: Generalized evolution equations for nonlinear surface gravity waves over two-dimensional topography, J. Fluid Mech. **552**, 393–418 (2006)
4.23 J.C.W. Berkhoff: Computation of combined refraction-diffraction, Proc. 13th Int. Conf. Coast. Eng. (1972) pp. 471–490
4.24 Z. Demirbilek, V. Panchang: *CGWAVE: A Coastal Surface Water Wave Model of the Mild Slope Equation*, Tech. Rep., Vol. CHL-98-26 (US Army Engineer Research and Development Center, Vicksburg 1998)
4.25 A.C. Radder: On the parabolic equation method for water wave propagation, J. Fluid Mech. **95**, 159–176 (1979)
4.26 J.T. Kirby: Higher-order approximations in the parabolic equation method for water waves, J. Geophys. Res. **91**, 933–952 (1986)
4.27 Y. Tang, Y. Ouellet: A new kind of nonlinear mild-slope equation for combined refraction-diffraction of multi-frequency waves, Coast. Eng. **31**, 3–36 (1997)
4.28 J. McCowan: On the highest wave of permanent type, Philos. Mag. **38**, 351–358 (1894)
4.29 R. Miche: Mouvements ondulatoires de la mer en profondeur constante ou decroissante, Ann. Ponts Chaussees **114e**, 42–78 (1944)
4.30 R.J. Weggel: Maximum breaker height, J. Waterw. Port Coast. Ocean Eng. **98**, 529–548 (1972)
4.31 B. Le Mehaute: On non-saturated breakers and the wave runup, Proc. 8th Int. Conf. Coast. Eng. (1962) pp. 77–92
4.32 K. Horikawa, C.-T. Kuo: A study of wave transformation inside surf zone, Proc. 7th Int. Conf. Coast. Eng. (1966) pp. 217–233
4.33 W.R. Dally, R.G. Dean, R.A. Dalrymple: Wave height variation across beaches of arbitrary profile, J. Geophys. Res. **90**, 11917–11927 (1985)
4.34 J.A. Battjes: Set-up due to irregular waves, Proc. 13th Int. Conf. Coast. Eng. (1972) pp. 1993–2004
4.35 Y. Goda: Irregular wave deformation in the surf zone, Coast. Eng. Japan **18**, 13–26 (1975)
4.36 J.A. Battjes, J.P.F.M. Janssen: Energy loss and set-up due to breaking of random waves, Proc. 16th Int. Conf. Coast. Eng. (1978) pp. 569–587
4.37 M.S. Longuet-Higgins: On the statistical distributions of sea waves, J. Mar. Res. **11**, 245–265 (1952)
4.38 E.B. Thornton, R.T. Guza: Transformation of wave height distribution, J. Geophys. Res. **88**, 5925–5938 (1983)

4.39 Y. Eldeberky, J.A. Battjes: Spectral modeling of wave breaking: Application to Boussinesq equations, J. Geophys. Res. **101**, 1253–1264 (1996)

4.40 T.T. Janssen, J.A. Battjes: A note on wave energy dissipation over steep beaches, Coast. Eng. **54**, 711–716 (2007)

4.41 T.E. Baldock, P. Holmes, S. Bunker, P. van Weert: Cross-shore hydrodynamics within an unsaturated surf zone, Coast. Eng. **34**, 173–196 (1998)

4.42 G. Symonds, D.A. Huntley, A.J. Bowen: Two-dimensional surf beat: Long wave generation by a time-varying breakpoint, J. Geophys. Res. **87**, 492–498 (1982)

4.43 B. Gallagher: Generation of surf beat by nonlinear wave interactions, J. Fluid Mech. **49**, 1–20 (1971)

4.44 A.J. Bowen, R.T. Guza: Edge waves and surf beat, J. Geophys. Res. **83**, 1913–1920 (1978)

4.45 I.A. Svendsen: *Introduction to Nearshore Hydrodynamics* (World Scientific, Singapore 2006)

4.46 D.A. Huntley, R.T. Guza, E.B. Thornton: Field observations of surf beat. 1. Progressive edge waves, J. Geophys. Res. **86**, 6451–6466 (1981)

4.47 F. Ursell: Edge waves on a sloping beach, Proc. R. Soc. Lond. Ser. A **214**, 79–97 (1952)

4.48 W.H. Munk: Surf beats, Trans. Am. Geophys. Union **30**, 849–854 (1949)

4.49 M.J. Tucker: Surf beats: Sea waves of 1 to 5 min period, Proc. R. Soc. Lond. Ser. A **202**, 565–573 (1952)

4.50 M.S. Longuet-Higgins, R.S. Stewart: Radiation stresses in water waves – A physical discussion, with applications, Deep Sea Res. **11**, 529–562 (1964)

4.51 J.H. List: A model for the generation of two-dimensional surf beat, J. Geophys. Res. **97**, 5623–5635 (1992)

4.52 M.A. Foda, C.C. Mei: Nonlinear excitation of long-trapped waves by a group of short swells, J. Fluid Mech. **111**, 319–345 (1981)

4.53 H.A. Schäffer, I.A. Svendsen: Surf beat generation on a mild-slope beach, Proc. 21st Int. Conf. Coast. Eng. (1988) pp. 1058–1072

4.54 S. Elgar, T.H.C. Herbers, M. Okihiro, J. Oltman-Shay, R.T. Guza: Observations of infragravity waves, J. Geophys. Res. **97**, 15573–15577 (1992)

4.55 A.R. Van Dongeren, I.A. Svendsen: Nonlinear and 3D effects in leaky infragravity waves, Coast. Eng. **41**, 467–496 (2000)

4.56 T.T. Janssen, J.A. Battjes, A.R. van Dongeren: Long waves induced by short-wave groups over a sloping bottom, J. Geophys. Res. **108**, 3252–3264 (2003)

4.57 J.A. Battjes, H.J. Bakkenes, T.T. Janssen, A.R. van Dongeren: Shoaling of subharmonic gravity waves, J. Geophys. Res. **109**, C02009 (2004)

4.58 J. Oltman-Shay, P.A. Howd, W.A. Birkemeier: Shear instabilities of the mean longshore current: 2. Field observations, J. Geophys. Res. **94**, 18031–18042 (1989)

4.59 A.J. Bowen, R.A. Holman: Shear instabilities of the mean longshore current: 1. Theory, J. Geophys. Res. **94**, 18023–18030 (1989)

4.60 A.J.H.M. Reniers, J.A. Battjes, A. Falques, D.A. Huntley: A laboratory study on the shear instability of longshore currents, J. Geophys. Res. **102**, 8597–8609 (1997)

4.61 N. Dodd, A. Falques: A note on spatial modes in longshore current shear instabilities, J. Geophys. Res. **101**, 22715–22726 (1996)

4.62 V.I. Shrira, V.V. Voronovich, N.G. Kozhelupova: Explosive instability of vorticity waves, J. Phys. Oceanogr. **27**, 542–554 (1997)

4.63 F. Feddersen: Weakly nonlinear shear waves, J. Fluid Mech. **372**, 71–91 (1998)

4.64 D.N. Slinn, J.S. Allen, P.A. Newberger, R.A. Holman: Nonlinear shear instabilities of alongshore currents over barred beaches, J. Geophys. Res. **103**, 18357–18379 (1998)

4.65 H.T. Özkan-Haller, J.T. Kirby: Nonlinear evolution of shear instabilities of the longshore current: A comparison of observations and computations, J. Geophys. Res. **104**, 25953–25984 (1999)

4.66 R.W. Yeung: Numerical methods for free-surface flows, Annu. Rev. Fluid Mech. **14**, 395–442 (1982)

4.67 M.A. Grosenbaugh, R.W. Yeung: Nonlinear free-surface flow at a two-dimensional bow, J. Fluid Mech. **209**, 57–75 (1989)

4.68 D.G. Dommermuth, D.K.P. Yue, W.M. Lin, R.J. Rapp, E.S. Chan, W.K. Melville: Deep-water plunging breakers: A comparison between potential theory and experiments, J. Fluid Mech. **189**, 423–442 (1988)

4.69 T. Vinje, P. Brevig: Nonlinear ship motion, Proc. 3rd Int. Conf. Numer. Ship Hydrodyn., Paris (1981)

4.70 O. Saout, P. Ananthakrishnan: Hydrodynamic and dynamic analysis to determine the stability of an underwater vehicle near a free surface, Appl. Ocean Res. **33**, 158–167 (2011)

4.71 P. Ananthakrishnan: Effects of viscosity and free-surface nonlinearity on the wave motion generated by an oscillating twin-hull, Proc. OMAE 31st Int. Conf. Ocean Arct. Offshore Eng., Rio de Janeiro (2012) pp. 279–288

4.72 M. Xue: Xu H. Yue D. K. P.: Computations of fully nonlinear three dimensional wave-wave and wave-body interaction: Part 1. Dynamics of steep three dimensional wave, Journal of Fluid Mechanics **438**, 11–39 (2001)

4.73 J.R. Morison, M.P. O'Brien, J.W. Johnson, S.A. Schaaf: The force exerted by surface waves on piles, Petroleum Trans. **189**, 149–154 (1950)

4.74 T. Sarpkaya, M. Isaacson: *Mechanics of Wave Forces on Offshore Structures* (Van Nostrand Reinhold Co., New York 1981)

4.75 R. McCamy, R. Fuchs: *Wave forces on piles: A diffraction theory*, Tech. Memo, Vol. 69 (US Army Corps of Engineers, Washington 1954)

4.76 C.C. Mei: *The Applied Dynamics of Ocean Surface Waves* (World Scientific, Singapore 1989)

4.77 P. Ferrant, K. Pelletier: Second order wave diffraction patterns about complex offshore structures, Proc. 10th Int. Conf. Offshore Polar Eng., Vol. 3 (2000) pp. 686–693